

University of Nevada, Reno

**Remotely Sensed Estimates of Evapotranspiration in Agricultural Areas of
Northwestern Nevada:**

Drought, Reliance, and Water Transfers

A thesis submitted in partial fulfillment of the requirements for the degree of

Master of Science in Geography

by

Matthew Bromley

Thomas Albright Ph.D. - Thesis Advisor

December 2015



THE GRADUATE SCHOOL

We recommend that the thesis
prepared under our supervision by

MATTHEW BROMLEY

Entitled

**Remotely Sensed Estimates Of Evapotranspiration In Agricultural Areas Of
Northwestern Nevada:
Drought, Reliance, And Water Transfers**

be accepted in partial fulfillment of the
requirements for the degree of

MASTER OF SCIENCE

Thomas Albright Ph.D. , Advisor

Kate Berry Ph.D., Committee Member

Justin Huntington Ph.D., Graduate School Representative

David W. Zeh, Ph.D., Dean, Graduate School

December, 2015

Abstract

The arid landscape of northwestern Nevada is punctuated by agricultural communities that rely on water primarily supplied by the diversion of surface waters and secondarily by groundwater resources. Annual precipitation in the form of winter snowfall largely determines the amount of surface water that is available for irrigation for the following agricultural growing season. During years of insufficient surface water supplies, particular basins can use groundwater in order to meet irrigation needs. The amount of water used to irrigate agricultural land is influenced by land use changes, such as fallowing, and water right transfers from irrigation to municipal use. To evaluate agricultural water consumption with respect to variations in weather, water supply, and land use changes, monthly estimates of evapotranspiration (ET) were derived from Landsat multispectral optical and thermal imagery over a eleven-year period (2001 to 2011) and compared to variations in weather, water supply, and land use across four hydrographic areas in northwestern Nevada.

Monthly ET was estimated using a land surface energy balance model, Mapping EvapoTranspiration at high Resolution with Internalized Calibration (METRIC), using Landsat 5 and Landsat 7 imagery combined with local atmospheric water demand estimates. Estimates of net ET were created by subtracting monthly precipitation from METRIC-derived ET, and seasonal estimates were generated by combining monthly ET for April-October (the regional agricultural growing season). Results highlight that a range of geographic, climatic, hydrographic, and anthropogenic factors influence ET. Hydrographic areas such as Mason Valley have the ability to mitigate deficiencies in surface water supplies by pumping supplemental groundwater, thereby resulting in low annual variability in ET. Conversely, the

community of Lovelock has access to limited upstream surface water storage and is restricted by groundwater that is saline and unsuitable for irrigation use. These factors result in Lovelock being extremely susceptible to instances of prolonged drought, and exhibiting large fluctuations in annual ET. This work clearly illustrates that agricultural consumptive use is a function of water supply, weather, and land use change, which is useful in distinguishing how prolonged droughts and changing climate will potentially affect different hydrographic areas and agricultural communities in the future.

Contents

Abstract.....	i
Figures.....	iv
Tables.....	vi
Introduction.....	1
Objectives	4
Study Area and Geographic Setting.....	6
Approach.....	8
Methods.....	11
Weather Data QAQC, ET _r Estimation, and Bias Correction.....	12
Image Preparation and Land Cover	15
METRIC Model	18
Application and Post Processing.....	25
Results.....	26
Discussion	36
Conclusions.....	42
Bibliography	43
Appendix: Tables of Monthly Evapotranspiration	49

Tables

Table 1 - Meteorological stations used to calculate ET_r and to bias correct gridded weather products.....	13
Table 2 - Monthly correction factors developed from the comparison of the METDATA ET_r product to ET_r calculated from the Lovelock SCAN weather station.	15
Table 3 - Comparison of NVET estimates, with calculated ET from this study	40
Table 4 – Monthly evapotranspiration for the Mason Valley study area for the years of study. .	49
Table 5 – Monthly evapotranspiration for the Fallon study area for the years of study.....	49
Table 6 – Monthly evapotranspiration for the Lovelock study area for the years of study.....	50
Table 7 – Monthly evapotranspiration for the Fish Springs Ranch study area for the years of study.....	50

Figures

Figure 1 – Image of northwestern Nevada, depicting the location of study areas and relevant features. Inset image depicts the four Landsat scenes that were used for this study (Background image acquired from MODIS).	3
Figure 2 – Detail image of study areas. (A) Fallon (B) Mason Valley (C) Lovelock (D) Fish Springs Ranch. (Landsat false color 5,4,1 - 2001).....	5
Figure 3 - Meteorological stations used to calculate ET_r and to bias correct gridded weather products (A) Fallon, Nevada Agrimet (B) Lovelock NNR SCAN (C) CIMIS-Buntingville #57. 12	12
Figure 4 - Values of Solar radiation (R_s) vs. Theoretical clear-sky solar radiation (A) Prior to correction (B) After correction	13
Figure 5 - ET_r derived from METDATA vs. ET_r derived from Lovelock SCAN.....	14
Figure 6. – The presence of clouds within images is noticeable in (A) true color image. (B) False color image used to enhance the appearance of clouds and shadows in order to manually create a mask to obscure affected areas. (C) The result of cloud masking with Green area representing the area that is omitted from future calculations.....	16
Figure 7- Agricultural area near Topaz Ranch Estates, NV where (A) a field irrigated by traditional means (2001) was converted to a (B) center-pivot irrigation system (2011).	17
Figure 8 - Data used to create ET estimates for a single agricultural field within Mason Valley, NV (2003) (A) ET_r (B) ET_rF (C) ET	24
Figure 9 –Agricultural polygons adapted from CLU data and used to spatially aggregate ET calculations.	26
Figure 10 - (A) Annual ET, (B) Annual precipitation, (C) Annual net ET for each study area, during the period of study.	27
Figure 11- Mean annual ET and annual net ET for each area of study. Upper and lower bars illustrate respective maximum and minimums for each study area.	28
Figure 12 - Mean seasonal ET and seasonal net ET for each area of study. Upper and lower bars illustrate respective maximum and minimums for each study area.	29
Figure 13 - Monthly ET for Mason Valley, Fallon, Lovelock, and Fish Springs Ranch	30
Figure 14 - Comparison of seasonal ET in Mason Valley for (A) 2002, in which the area received below average precipitation and surface water deliveries, and (B) 2006, which was not restricted by water.....	32

Figure 15 - Comparison of seasonal ET for Fallon, NV for (A) 2009, in which the area received below average precipitation and surface water deliveries, and (B) 2010, which was not restricted by water.....	33
Figure 16 - Comparison of ET for Lovelock, NV. (A) 2004 represents a period affected by an occurrence of multi-year drought, while (B) 2006 is provided adequate water, due to the replenishment of water resources.....	34
Figure 17 - Comparison of ET for Fish Springs Ranch for (A) 2002, while irrigation was conducted and (B) 2009, after groundwater rights were converted to municipal use and irrigation ceased.....	35
Figure 18 - ET estimates from this study are compared to estimates by NVET (Huntington and Allen, 2010). Maximum and minimum rates of annual ET are represented with upper and lower bars.....	41
Figure 19 - Comparison of mean daily flows of the Carson River (USGS 10312150 CARSON RV BLW LAHONTAN RESERVOIR NR FALLON, NV)	37
Figure 20 - Comparison of mean daily flows of the Humboldt River (USGS 10335000 HUMBOLDT RV NR RYE PATCH, NV).....	38

Introduction

Irrigated agriculture is practiced within arid regions worldwide. For these agricultural communities, water demands generally exceed precipitation, thus requiring more water than is immediately available. Natural and manmade reservoirs have been used in conjunction with diversions of various kinds, in order to deliver water when and where it is needed.

For many locations, the annual rhythm of depletion and recharge of reservoirs does not allow for sufficient storage of water to fully sustain agriculture for multiple seasons. Consequently, prolonged drought and water scarcity pose significant hazards to these areas; one such area is northwestern Nevada. According to the Fifth Assessment Report of the Intergovernmental Panel on Climate Change (IPCC), it is projected that many areas, including the western United States, will experience increased occurrences of drought [Barros *et al.*, 2014]. Changing precipitation regimes associated with a changing climate may also result in complications to established strategies of providing water.

The arid landscape of northwestern Nevada (Figure 1) is punctuated by agricultural communities that primarily rely on the diversion of surface waters and secondarily depend on groundwater resources. The amount of surface water available for diversion is generally dependent on annual climate variability. During periods when surface water is insufficient, groundwater is utilized by some areas to supplement surface water supplies. The practice of pumping supplemental groundwater is dependent on several factors, including location, water rights, and groundwater quality (for example, high levels of salinity). The amount of irrigation water applied is influenced by crop and soil type, atmospheric demand, and alterations in land use and changes in

the allocation and the manner of use (i.e. water rights transfers from agricultural irrigation to municipal uses).

In preparing for the scarcity of water associated with multi-year drought, various strategies may be employed, such as deficit irrigation or procuring additional water through interbasin transfers. Further methods of mitigating drought without adversely affecting groundwater resources or building reservoirs for the capture and retention of surface water are extremely limited.

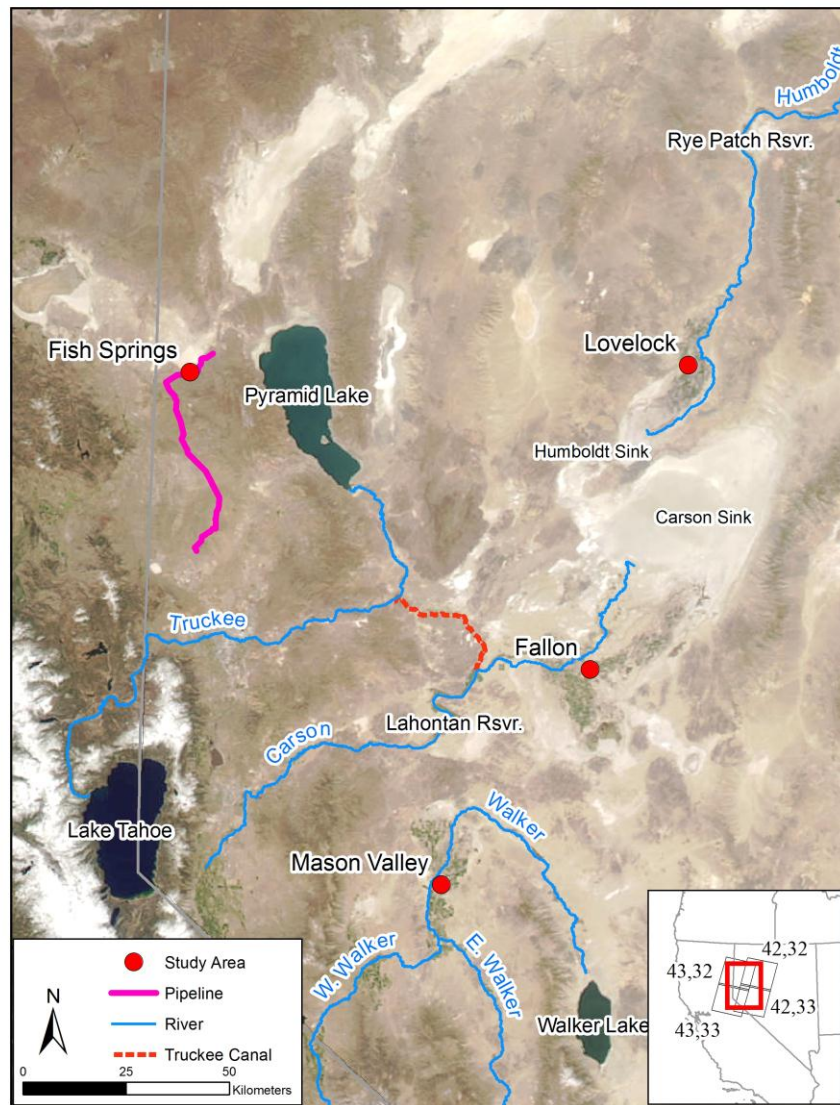


Figure 1 – Image of northwestern Nevada, depicting the location of study areas and relevant features. Inset image depicts the four Landsat scenes that were used for this study (Background image acquired from MODIS).

Depending on the water source and water rights structure (i.e. federal decree, State of Nevada water law), the impacts of water scarcity can differ considerably from one hydrographic area (HA) to another. Because agricultural yield is highly correlated to consumptive water use [Guitjens and Goodrich, 1994], estimating the consumptive water use of agriculture in the form of evapotranspiration (ET) can be an effective approach to assess the impacts of drought,

variability in water source, and land use change in agricultural communities. In addition to examining recent patterns of ET, evaluating the recent consumptive use of water in agriculture may allow for improved water and risk management.

Evapotranspiration (ET) is the combined processes of water lost from the soil surface by evaporation and water lost from the stomata of plants through transpiration. Because evaporation and transpiration take place simultaneously and through similar mechanisms, it is difficult to segregate the water vapor that is produced from the two processes [Dingman, 2008]. Several factors affect ET including weather, management practices, environmental conditions and plant characteristics. ET is mechanistically driven by components of weather such as solar radiation, air temperature, humidity and wind speed. Conversely, limitations in water availability, high soil salinity, nutrient deficiencies, lack of pest control, and poor soil management can suppress productivity of agricultural vegetation and therefore suppress the rates of ET [Allen *et al.*, 1998a; Katerji *et al.*, 1998].

Objectives

The overarching objective of this work is to demonstrate the utility of remotely sensed ET estimates in characterizing seasonal, annual, and geographic differences in ET rates related to weather, water source, and land use practices. Specific questions I addressed include: 1) How does the consumption of water (ET) vary based on water availability during wet and dry years? 2) What is the relationship between ET and access to surface water or groundwater sources? 3) How has land-use change associated with water rights transfers influenced agricultural water consumption?

To answer these questions, I evaluated monthly, seasonal, and annual totals of ET from agricultural areas in four different HAs across northwestern Nevada over a eleven-year period (2001-2011). This period includes both multi-year drought and years receiving above average precipitation.

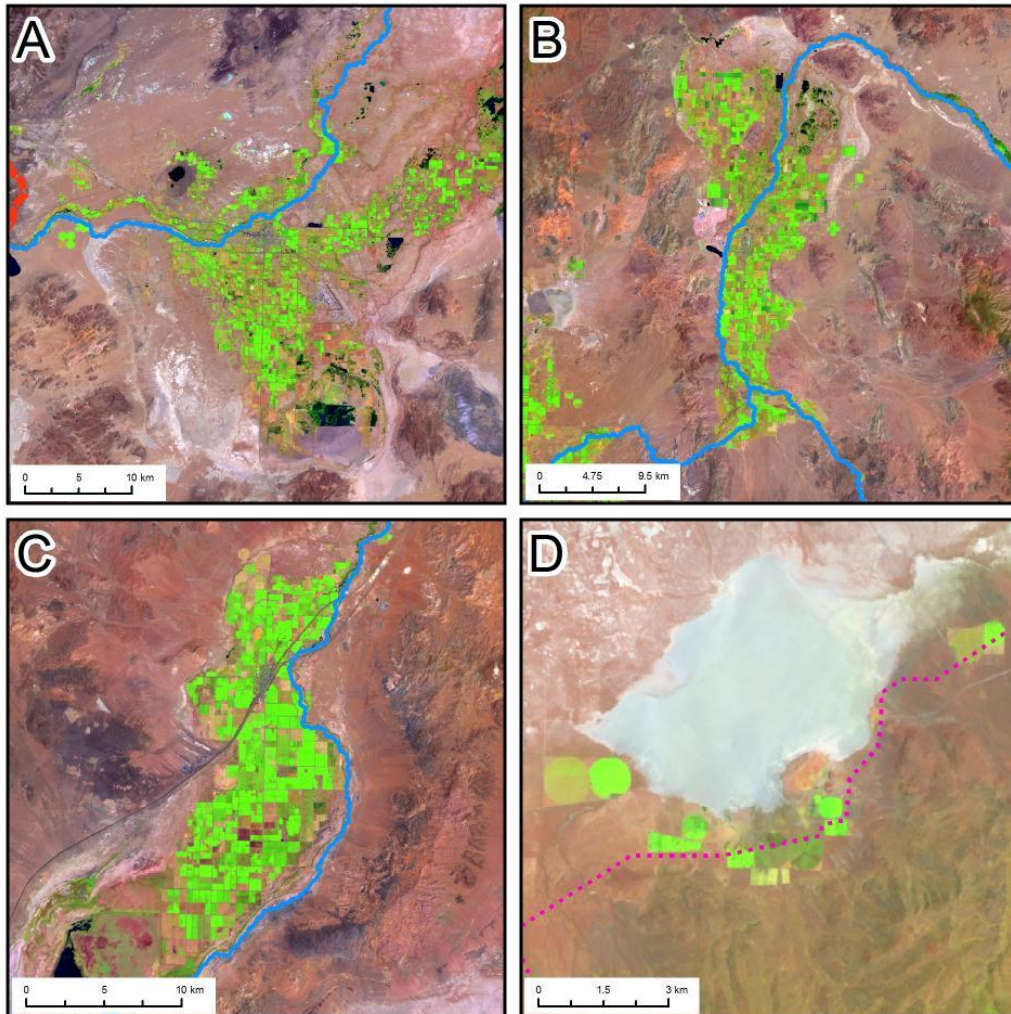


Figure 2 – Detail image of study areas. (A) Fallon (B) Mason Valley (C) Lovelock (D) Fish Springs Ranch.

(Landsat false color 5,4,1 - 2001).

Study Area and Geographic Setting

The study areas selected for the analysis were composed of the agricultural communities of Lovelock, Fallon, Mason Valley, and Fish Springs Ranch (Figure 2). These areas within northwestern Nevada were selected based on having a wide range of physical characteristics related to water source, surface water availability, groundwater quality, and land-use change. The climate within the study area is dominantly characterized as arid to semi-arid, receiving mean annual precipitation ranging from 100 to 250 mm, with approximately 80% of the precipitation occurring during the winter months. The hottest month is July with an average high of 33 °C, contrasted with December, with an average low of -10 °C. The agricultural areas are surrounded by rangeland that comprises spatially extensive and homogenous phreatophytic and xerophytic shrub species. The assemblage of species is largely dependent on soil conditions and may include combinations of greasewood (*Sarcobatus vermiculatus*), salt grass (*Distichlis spicata*), rabbitbrush (*Ericameria nauseosa*), and sagebrush (*Artemisia tridentata*). Alfalfa (*Medicago sativa*) comprises approximately 90% of the agricultural study areas, with marginal amounts of spring and winter grain, corn, potatoes, onions, and garlic [USDA National Agricultural Statistics Service and Service, 2015]. Alfalfa in Nevada is often exported to dairy farms in California, and internationally [Nevada Department of Agriculture, 2015].

The agricultural water supply for the community of Lovelock is entirely dependent on the Humboldt River, where water is applied through the application of flood irrigation. Rye Patch Reservoir provides limited upstream storage for irrigation throughout the agricultural growing season. Due to the limited capacity of the reservoir (213,000 acre-feet of water storage [Hoffman et al., 1990]), releases of water from Rye Patch Dam during periods of multi-year drought may

diminish to zero (Figure 20). Lovelock is located nearest to the study area of Fallon, NV with both areas located at the terminus of river systems, the Humboldt Sink and the Carson Sink, respectively. The location of these communities in relation to the river systems results in the nearby groundwater being largely unsuitable for irrigation due to high salinity. This restriction dictates that both agricultural communities rely on the annual flows of surface water and upstream storage maintained in reservoirs [Everett and Rush, 1965; Truckee-Carson Irrigation District, 2010]. The agricultural community of Fallon benefits from larger surface water storage within Lake Lahontan (312,900 acre-feet of storage [Truckee-Carson Irrigation District, 2010]) and access to the flows of the Carson River and the Truckee River via the Truckee Canal. This diversion, which was built as part of the Newlands Project in 1905, allows Fallon to benefit from the robust storage of water within the Truckee River system. This storage includes Lake Tahoe and several other reservoirs of smaller capacity (i.e. Donner and Independence Lakes, and Boca, Stampede, Prosser, and Martis Reservoirs) [Berris et al., 2001]. Irrigation in the Fallon area is applied through flood irrigation and wheel line sprinklers.

Mason Valley is unique among the study areas in that the Walker River transects the valley, providing readily available access to surface water. The Walker River provides the benefit of upstream water storage within Topaz Lake (59,440 acre-ft of storage capacity [Rush and Hill, 1972]). Many of the water users within the valley hold both surface water and supplemental groundwater rights, where groundwater may be used during periods when the Walker River is regulated by water right priority, resulting in the curtailment of water for low priority surface water right holders [Carroll et al., 2010]. During periods of extended drought, supplemental groundwater pumping may become the primary source of water in order to meet irrigation water

demands. Irrigation for Mason Valley is comprised of a mix of flood irrigation, wheel line sprinklers, and center pivot irrigation.

Located in the Honey Lake Basin, Fish Springs Ranch has primarily used groundwater to irrigate crops with a combination of center pivot irrigation and wheel line sprinklers. In 2000, Fish Springs Ranch was acquired by a private company as a means to procure 13,000 acre-feet of fully permitted groundwater rights associated with the property [*Vidler Water Company*, 2015]. In 2009, construction was completed on a pipeline to be used to transport groundwater to Lemmon Valley, in suburban Reno. The transfer of water was delayed due to the onset of negative economic conditions, which stalled the construction of new housing and thereby decreased the demand for additional and diversified sources of municipal water. As of 2015, improved economic conditions will likely result in future inter-basin transfers of water [*DeLong*, 2015].

Approach

Recent advances in remote sensing and computational research using Landsat satellite imagery and gridded weather data for mapping field scale ET have provided an excellent opportunity for improving our understanding of historical water use of irrigated environments [*Anderson et al.*, 2012]. The minimal resolution needed to discriminate agricultural features, and therefore perform calculation relevant to water rights and environmental assessments, is approximately 100 meters [*Anderson et al.*, 2012; *Yan and Roy*, 2016]. Landsat imagery, which was made freely available to the public as of 2009, has a native spatial resolution of 30 m for optical channels and up to 120 m for thermal channels. In temperate latitudes, any geographic location is generally visible by

Landsat images at a 16-day interval from Landsat 5, and at an 8-day interval when combined with Landsat 7. While the fidelity of calculations improves with coverage of two remote sensing platforms, the temporal resolution provided by a single Landsat platform is sufficient to track crop phenology and seasonality of water usage, and agricultural practices such as alfalfa cuttings and annual crop harvests [Tasumi *et al.*, 2005; Cammalleri *et al.*, 2014]. The study period includes several years when both Landsat 5 and Landsat 7 were fully functional, resulting in an increase in the total number of scenes unobscured by cloud cover, thus creating more accurate estimates of ET.

Due to the arid climate and minimal cloud cover of northwestern Nevada, the probability of obtaining at least one cloud free image every 32 days, at a 8 and 16 day return intervals is high, ranging from 50 to 95 percent, respectively [Morton *et al.*, 2015a]. The high spatial resolution of Landsat allows scientists, policy makers, and resource managers to identify field-scale crop water use, and within-field variability [Tasumi *et al.*, 2005; Tasumi and Allen, 2007].

This approach for calculating ET relies on estimating the land surface energy balance from imagery acquired by the Landsat TM and ETM+ sensors, and locally measured or modeled weather data. This data is utilized within the METRIC model [Allen *et al.*, 2007; Anderson *et al.*, 2012]. Vegetation indices, land use / land cover, surface temperature, and reference ET (i.e. atmospheric water demand) are the primary variables driving the METRIC surface energy balance approach, as well as being the primary factors in influencing ET over time. In this regard, METRIC offers spatially explicit actual ET estimates that are accurate to within 10-20% [Allen *et al.*, 2007; Kalma *et al.*, 2008]. The METRIC approach has been applied in Nevada with much success by Morton *et al.* [Morton *et al.*, 2013] and Huntington *et al.* [Huntington *et al.*,

2014], with the results from these studies comparing well with micrometeorological estimates of crop ET in Nevada. METRIC has also been recently applied by several state and federal agencies for estimating ET from agricultural lands in Nevada, New Mexico, Oregon, Wyoming, Montana, Nebraska, Colorado, and California [*Hendrickx, 2010; Kjaersgaard and Allen, 2010; Anderson et al., 2012; Snyder et al., 2012; Serbina and Miller, 2014; Morton et al., 2015b*].

In addition to agricultural weather station data, bias-corrected and spatially disaggregated North American Land Data Assimilation System gridded weather data, METDATA [*Abatzoglou, 2013*] provide daily maximum and minimum air temperature (T_{\max} and T_{\min}), daily maximum and minimum relative humidity (RH_{\max} and RH_{\min}), dew point temperature (T_{dew}), solar radiation (R_s) and daily average wind speed at a 2m height (u_2). These values were used to estimate daily reference ET (ET_r) for each study area (Figure 3). Daily ET_r is used in the METRIC process to perform time integration of actual ET between Landsat image acquisitions to develop daily, monthly, and seasonal ET distributions (For the purposes of this study, “seasonal” is defined as the agricultural growing season from April through October). Precipitation data derived from the Parameter Regression on Independent Slopes Model (PRISM; *Daly et al. [2002]*) at 800-m spatial resolution are used for estimating monthly precipitation and net ET (ET minus precipitation) for each study area.

Monthly METRIC ET estimates are summarized and spatially averaged to agricultural field boundaries derived from Common Land Unit (CLU) data [*USDA Farm Service Agency, 2012*] and manually modified for each year to reflect changes in land use. Finally, spatially averaged rates of ET for agricultural fields within each study are summarized and compared based on respective inter-annual climate variability, water sources, and land use changes. In addition to

demonstrating that agricultural consumptive use is a function of water source and supply, climate, and the reallocation of water, results summarized in this work have a variety of uses ranging from supporting legal findings of fact, water rights compliance, monitoring and mitigation, water rights leasing and purchasing agreements, hydrological modeling, refining basins budgets, and water planning.

Free access to the entire Landsat archive combined with publically available weather station and gridded weather data has provided the unique capability to develop a reproducible time series of field-scale ET for a large area within northwestern Nevada, utilizing publicly available data. This result is not possible to obtain through ET measurements utilizing in-situ data collection.

Methods

Estimating actual ET from Landsat and weather data required numerous stages of data processing, and quality assurance and control (QAQC) procedures that are described below. Landsat TM and ETM+ images were acquired for the study period of 2001-2011 from the U.S. Geological Survey (USGS) Global Visualization web page (<http://glovis.usgs.gov/>), totaling 412 scenes. Landsat data was processed to top-of-atmosphere reflectance following the protocol outlined by Chandler and Markham. [2003] through the application of Python scripting, many of these scripts are described by Morton et al. [2013]. The following subsections describe methods used for weather data QAQC and bias correction, image preparation and cloud masking, land use classification, the utilization of the METRIC model, and the summarizing of results.

Weather Data QAQC, ET_r Estimation, and Bias Correction

I performed extensive QAQC of measured agricultural weather data (Figure 3; Table 1) prior to image processing and the application of the METRIC model. Hourly and daily average variables of maximum temperature (T_{max}), minimum temperature (T_{min}), maximum relative humidity (RH_{max}), minimum humidity (RH_{min}), solar radiation (R_s), and the wind velocity at a 2-m height (u_2) were input into the software program, REF-ET [Allen, 2011]. This software was used to visualize, filter, and make necessary corrections to variables according to the recommendations and guidelines of Allen [1996], Allen et al. [2005], and Allen [2008]. Prior to the computation of ET_r , each variable was compared to theoretical limits such as clear sky solar radiation (Figure 4), 100 percent RH, and dew point depression ($T_{min} - T_{dew}$).

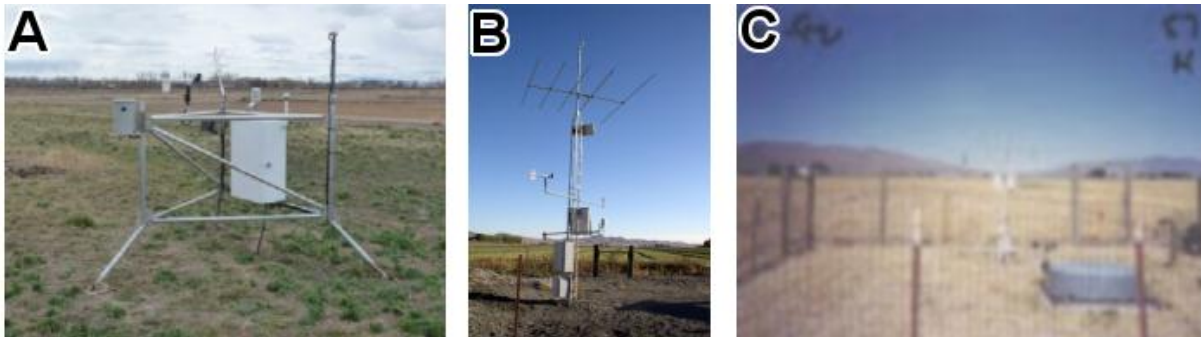
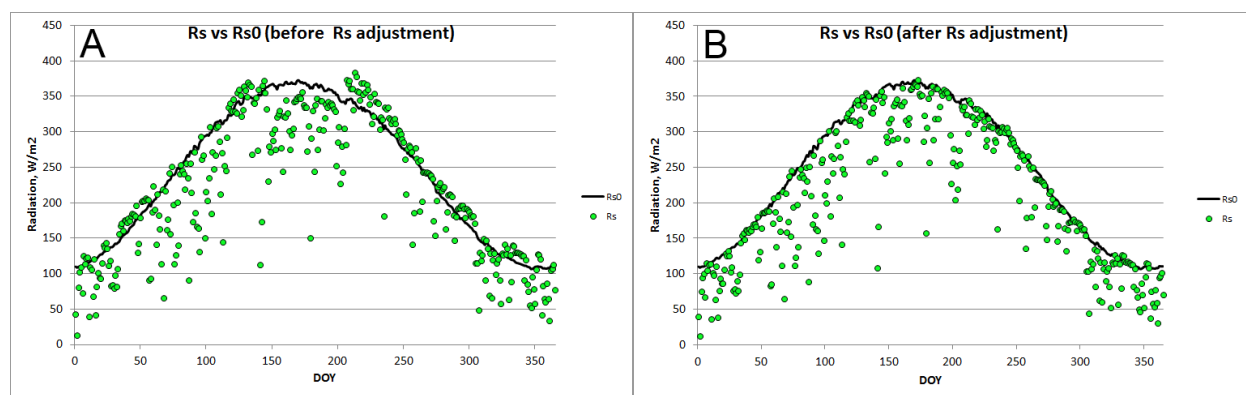


Figure 3 - Meteorological stations used to calculate ET_r and to bias correct gridded weather products (A) Fallon, Nevada Agrimet (B) Lovelock NNR SCAN (C) CIMIS-Buntingville #57.

Table 1 - Meteorological stations used to calculate ET_r and to bias correct gridded weather products.

Meteorological Stations Used to Calculate Referent Evapotranspiration						
Station	Network	Lat.	Long.	Elevation (ft)	Elev. (m)	Study Area
Fallon, Nevada AgriMet	AgriMet	39.458	-118.774	3965	1209	Fallon, NV & Mason Valley, NV
Lovelock NNR SCAN	Soil Climate Analysis Network (SCAN)	40.033	-118.183	3934	1199	Lovelock, NV
CIMIS - Buntingville #57	California Irrigation Management Information System (CIMIS)	40.290	-120.435	4005	1221	Fish Springs Ranch, NV

**Figure 4 - Values of solar radiation (R_s) vs. theoretical clear-sky solar radiation (A) prior to correction (B) after correction.**

Solar radiation measurement errors are most common, and occur due to debris on the pyranometer window, non-level base plate, sensor miscalibration or drift, or obstructions [Allen, 2008]. I calculated ET_r using QAQCed agricultural weather data from each study area weather station using the American Society of Civil Engineers Standardized Penmen-Monteith (ASCE-PM) reference ET equation (ASCE-EWRI, 2005). The Lovelock Soil Climate Analysis Network (SCAN) station measurement period of measurement was limited to a period of 2006 to present, with gaps in in the collection of suitable data for the years of 2007, 2010, and 2011. Due to the absence of weather data for the period of study, simulated daily variables were required for the ASCE-PM equation (T_{max} , T_{min} , RH_{max} , RH_{min} , R_s , and u_2). These necessary variables were obtained from the METDATA 4 km gridded weather dataset [Abatzoglou, 2013], and ET_r was

estimated using the ASCE-PM equation. Comparisons of daily ET_r computed with measurements from the SCAN station were made with 4-km grid cell METDATA derived ET_r for the period of 2001 to 2014. Daily time series results indicate that METDATA simulated weather compares fairly well to the Lovelock SCAN station. Comparison revealed that a small positive bias in METDATA ET_r was evident and varied seasonally (Figure 5).

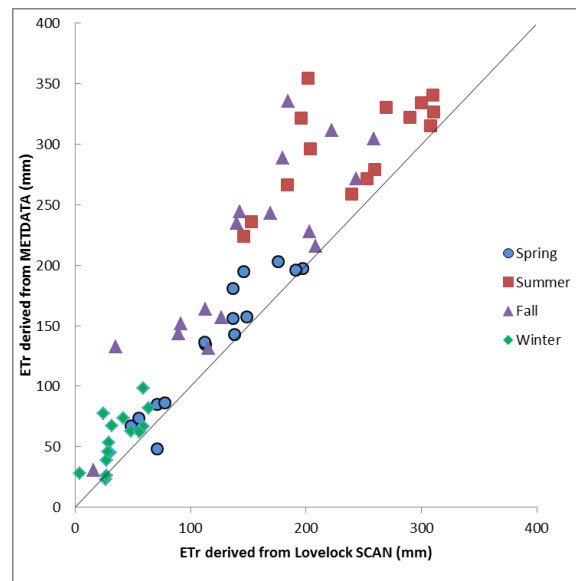


Figure 5 - ETr derived from METDATA vs. ETr derived from Lovelock SCAN.

This bias in METDATA ET_r is primarily attributed to gridded T_{max} , T_{min} , and T_{dew} being slightly warmer than the respective station measurements. A bias of this nature is typical when comparing simulated weather of an arid environment, to weather observations collected in a fairly well irrigated environment, such as the agricultural area surrounding the Lovelock SCAN station. In this case, the primary data source of METDATA, the North American Land Data Assimilation System [Rodell *et al.*, 2015; Mitchell *et al.*, 2004] does not account for irrigated areas and the enhancement of ET by land surface – boundary layer processes [Ozdogan and Rodell, 2010]. Even in advective arid environments like Northern Nevada, field-scale feedbacks

have been well documented in irrigated areas surrounded by water-limited regions [Allen *et al.*, 1983; Temesgen *et al.*, 1999; Szilagyi and Schepers, 2014; Huntington *et al.*, 2015]. Despite this common knowledge, practitioners and researchers alike routinely and erroneously apply ET_r equations to estimate well-irrigated crop ET using arid or non-conditioned weather data. In order to bias correct METDATA to estimate agricultural representative ET_r , mean monthly ratios of measured ET_r to METDATA ET_r were computed, and were multiplied by daily METDATA ET_r for respective months for the study period of record (2001-2011).

Table 2 - Monthly correction factors developed from the comparison of the METDATA ET_r product to ET_r calculated from the Lovelock SCAN weather station.

	JAN	FEB	MAR	APR	MAY	JUN	JUL	AUG	SEP	OCT	NOV	DEC
CORRECTION FACTOR	0.57	0.80	0.90	0.89	0.87	0.83	0.85	0.76	0.72	0.74	0.65	0.60

Weather data, such as daily precipitation (PPT), and daily ET_r , were used in a soil-water balance model [Allen *et al.*, 2011] to estimate rates of bare soil evaporation that are associated with rainfall prior to each Landsat image. Bare soil evaporation for the day of acquisition must be accounted for when implementing the calibration of METRIC at extreme conditions, discussed in the section “METRIC Model.” The soil-water balance model was parameterized based on soil type, available water capacity, soil water content at field capacity, and plant wilting point. Soil data used for defining these parameters were obtained from the NRCS SSURGO soils GIS database, and subset for agricultural areas [NRCS, 2015].

Image Preparation and Land Cover

To ensure that Landsat pixels were without smoke, haze, clouds, cirrus, shadows, cold air pooling, or image banding, it was necessary to visually inspect all available scenes within the

study period (412 scenes, wherein most scenes comprised two adjacent Landsat images within a single path). If scenes were too contaminated with clouds or distortions that obscured the agricultural areas, the scenes were not used. In the event that limited clouds or other contamination features were present, masks were manually created in order to omit these areas from the model. In order to facilitate the processing of the dataset, false color images utilizing visible, infrared, and thermal infrared bands of electromagnetic spectrum were used to enhance the appearance of clouds, shadows, cirrus, and haze.

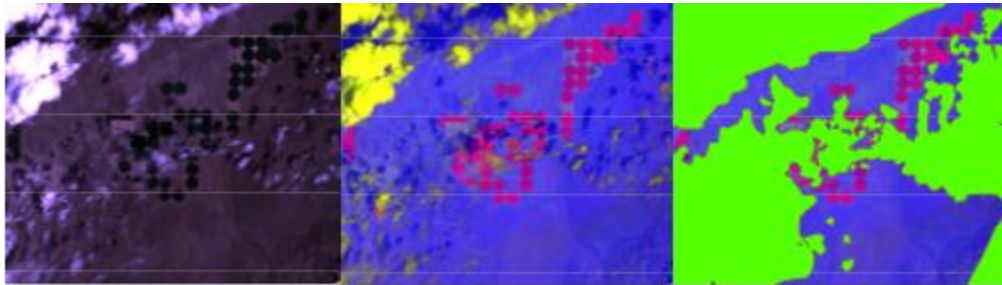


Figure 6 – The presence of clouds within images is noticeable in (A) true color image. (B) False color image used to enhance the appearance of clouds and shadows in order to manually create a mask to obscure affected areas. (C) The result of cloud masking with Green area representing the area that is omitted from future calculations.

Land cover information was required for parameterization of land surface roughness, emissivity, and energy balance functions in the METRIC model, and was additionally used to summarize ET results for each study area. The information pertaining to land cover was composed of two separate datasets. The first was a dataset of CLU agricultural polygons (CLU, 2008) that was modified to improve the accuracy of the dataset compared to agricultural areas within the study area. During years when NAIP was not available, Landsat false color composites were used in combination with NAIP imagery and National Land Cover Database (NLCD) data from adjacent years. For example, agricultural polygons developed for 2001 were used as the initial reference

for the development of the 2002 agricultural polygons. This process was repeated for 2002-2011 in order to carry over accuracy improvements from previous years. Improving the accuracy of land cover was necessary due to alterations in the agricultural boundaries that occurred during the study period. This was most often seen when traditional fields were converted to a center-pivot irrigation system (figure 7).

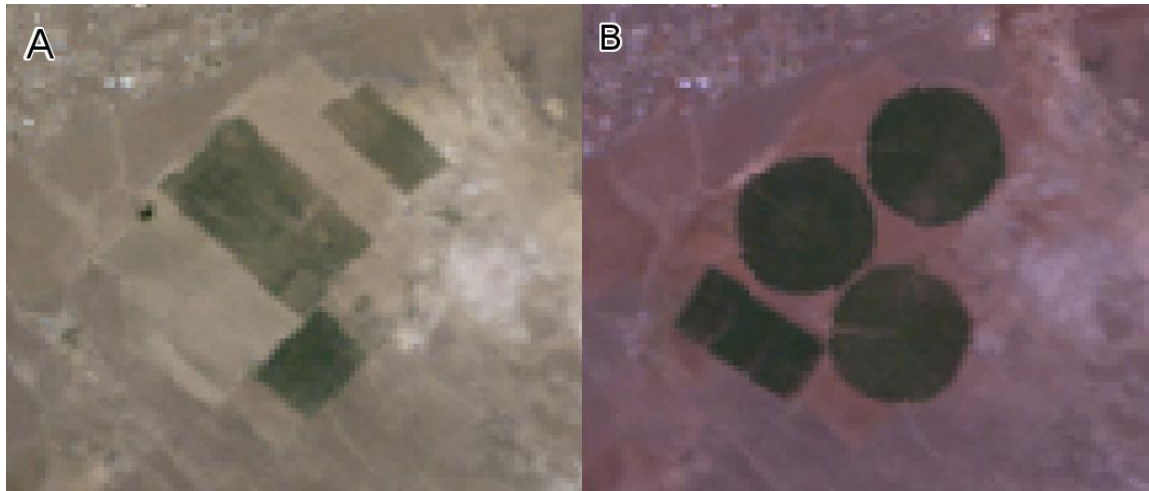


Figure 7- Agricultural area near Topaz Ranch Estates, NV where (A) a field irrigated by traditional means (2001) was converted to a (B) center-pivot irrigation system (2011).

Surface roughness in the METRIC model was estimated from land cover data derived from three versions of NLCD [*Homer et al.*, 2007, 2015; *Fry et al.*, 2011], representing the years 2001, 2006, and 2011. Detailed QAQC revealed that NLCD was not sufficiently accurate in representing land cover for the period of study due to misclassification and the omission of changes in land cover. The modified agricultural polygon dataset was used integrated with the agricultural land cover represented in the NLCD datasets, which resulted in a hybrid dataset that improved land cover accuracy for each year of the study period.

METRIC Model

Agricultural ET from 2001 to 2011 was estimated for each study area using METRIC. The METRIC model computes instantaneous ET for each Landsat pixel by estimating surface energy balance components and estimating latent heat flux as a residual of the energy balance as

$$LE = R_n - G - H$$

where LE is the flux of latent energy (W/m^2), R_n is the net radiation at the surface (W/m^2), G is the ground heat flux (W/m^2), and H is the sensible heat flux (W/m^2). METRIC estimates of R_n , G, and H are derived from hourly weather data, Landsat at-surface reflectance and thermal radiance, vegetation indices, and measured incoming solar radiation [Allen *et al.*, 2007, 2014]. Radiometric and atmospheric corrections to estimate at-surface reflectance, surface temperature, and albedo were made following Tasumi *et al.* [Tasumi *et al.*, 2008]. R_n is estimated using Landsat derived albedo, emissivity, and estimates of shortwave and longwave radiation. G is estimated as a function of land cover type, R_n , vegetation indices, and surface temperature. Sensible heat flux is estimated as a function of surface temperature and atmospheric stability using an iterative process, called the Calibration using Inverse Modeling at Extreme Conditions (CIMEC) procedure [Allen *et al.*, 2007]. The CIMEC process factors out many of the biases in the energy balance, especially in surface temperature, estimated R_n , and model assumptions [Allen *et al.*, 2007].

The CIMEC procedure requires two anchor pixels (i.e. calibration points), where ET is known, so that the energy balance can be solved for H at these locations that represent extreme conditions in the image. Once H is known at these locations, a linear relationship between Landsat surface temperature and the estimated temperature gradient, near surface air temperature

difference (dT), just above the land surface can be established and applied to the surface temperature image to estimate H , and therefore ET once R_n and G are estimated for every pixel in the image. Anchor point pixels, or “calibration points” for each image were manually selected based on a combination of image properties to guide selection representative of extreme ET conditions, such as surface temperature, the Normalized Difference Vegetation Index (NDVI), and albedo.

The “hot pixel” calibration point is representative of the condition where there is substantial surface heating due to the absence of evaporative cooling, relating to the absence or minimal occurrence of ET . This calibration point ideally represents a location composed of bare, dry agricultural soil and was additionally selected on the basis that the agricultural field containing the anchor point was homogenous within the field boundaries in regards to appearance, temperature, and albedo. The criteria used to select hot pixels prescribed followed recommendations in the METRIC manual [Allen *et al.*, 2014] and METRIC publication [Allen *et al.*, 2007]. Hot pixels selected most often exhibited a NDVI and an albedo within the range of 0.11 to 0.2, and 0.17 to 0.23, respectively.

The “cold pixel” calibration point is representative of the condition where maximum ET occurs. This condition is generally characterized as full vegetation cover, is well irrigated, and is at or near the alfalfa reference ET (ET_r) rate, where effectively all available energy (R_n-G) is being used for LE , and H is near or at zero. Full cover alfalfa typically exhibits an albedo in the range of 0.18 to 0.24 and NDVI range of 0.76 to 0.84 [Allen *et al.*, 2014]. These ranges are applicable for selecting cold pixels within images that were acquired during the growing season.

Images acquired early and late in the calendar year did not contain areas fully covered with agricultural vegetation. Therefore, cold pixels selected for this timeframe were selected utilizing a more relaxed criterion for albedo and NDVI. Estimates of early and late season ET are less sensitive to the criteria used for pixel selection due to low ET_r , therefore potential biases do not greatly affect monthly ET totals, and in this study early and late months are not included in seasonal ET totals. Cold pixels were optimally selected near the center of the agricultural field to prevent edge effects, and within fields that were surrounded by similar land cover in order to avoid a clothesline or oasis effect.

Once hot and cold calibration pixels were selected, respective ET rates were specified at each location. The ET rate at the cold pixel is typically assumed to be approximately 0 to 5 percent greater than the ET_r because the ET_r does not account for ET from a wet canopy or soil, due to recent irrigation [Tasumi *et al.*, 2005; Allen *et al.*, 2007]. The ET rate at the hot pixel is typically specified as 0 to 10 percent of the ET_r to account for residual water content and evaporation common in agricultural soils. Estimates of bare soil evaporation using the model of Allen *et al.* [2011] were incorporated to specify the hot pixel evaporation rate to account for any residual evaporation from rainfall events prior to acquisition of Landsat imagery. If residual evaporation was estimated to be above 10 percent of ET_r , then the hot pixel ET rate was specified according to the estimated fraction of ET_r provided by the bare soil evaporation model of Allen [Allen *et al.*, 2011].

Once hot and cold pixels were selected, the METRIC model (and internal CIMEC procedure) is used to estimate instantaneous R_n , G, H, and LE for every pixel in the image. The instantaneous rate of ET at the time of image acquisition, ET_{inst} (mm/hr), is calculated as

$$ET_{inst} = 3600 \times LE_{inst} / \lambda$$

where LE_{inst} is the instantaneous latent heat flux derived from METRIC (w/m^2), λ is the latent heat of vaporization for water (J/kg - i.e. the amount of energy absorbed when a kilogram of water evaporates), and 3600 is a factor for time conversion from seconds to hours. While the ET_{inst} is useful for many ecological and agricultural applications, such as detecting vegetation stress and water limitations, time integration of ET_{inst} to estimate monthly and seasonal water use is needed for water resource applications. Time integration requires that a temporal index of ET_{inst} be used to account for temporal variations in ET, caused by primarily by changes in vegetation phenology, weather, and climate. This temporal index is developed by relating ET_{inst} to the reference ET at the time of image acquisition (ET_{r_inst}). Hourly ET_r is time interpolated to the exact image acquisition time (usually between 10:30am to 11:00am PST) to estimate ET_{r_inst} . The ratio of ET_{inst} to ET_{r_inst} is termed the instantaneous fraction of reference ET (ET_rF), otherwise known as the “crop coefficient”. This ratio, which can be computed over many different time scales, is commonly used in agricultural engineering and hydrology to relate actual crop conditions to reference crop conditions in time and space [Allen *et al.*, 1998b]. Variability in ET_rF is the result of differences in water availability, vegetation growth stages and phenology changes, vegetation roughness and turbulent effects, and vegetation cover and geometry (i.e. full cover vs. row crops). Simply put, the effects of weather and climate are incorporated into ET_r , whereas the effects that distinguish vegetated and bare surfaces from the reference surface are integrated into the ET_rF [Allen *et al.*, 1998a; Hobbins and Huntington, 2015]. There are many physiological, physical, and climatological factors that determine ET, and the reference ET and

crop coefficient approach incorporates the majority of these factors [Allen *et al.*, 2005; Bos *et al.*, 2009]

Once $ET_r F$ was computed for every pixel in the image from spatially distributed ET_{inst} and ET_{r_inst} derived from the Fallon AgriMet weather station, the ET rate for a 24 hour period (ET_{24i}) (mm/d) was estimated as

$$ET_{24i} = ET_r F_i \times ET_{r_24i}$$

where ET_{r_24i} is the 24-hour ET_r total (mm/d) and $ET_r F_i$ is the fraction of ET_r for day i (dimensionless). As previously described, because satellite imagery only provides instantaneous information at the time of acquisition, daily ET_r is used to account for daily variations in atmospheric water demand (i.e. T_{max} , T_{min} , RH_{max} , RH_{min} , R_s , and u_2). Two major assumptions in this approach are 1) the ratio of ET_{inst} to ET_{r_inst} is fairly stable over a 24-hour period and/or the $ET_r F$ ratio at the time of image acquisition is approximately equal to the 24-hour value, and 2) daily ET is proportional to daily ET_r . These assumptions are generally met for agricultural vegetation due to limited regulation of stomatal conductance, photosynthesis and transpiration [McNaughton and Jarvis, 1991; Allen *et al.*, 1998a; Tolk and Howell, 2001; Hunsaker *et al.*, 2003; Cammalleri *et al.*, 2014]. Non-cultivated vegetation in riparian and desert vegetation systems, uses stomatal regulation of transpiration as a physiological water use strategy, thus affecting the hourly and daily $ET_r F$, especially under water-limited conditions [Schulze *et al.*, 1972; Collatz *et al.*, 1991; Liebert *et al.*, 2015]. Liebert *et al.* [2015] showed for a well-irrigated riparian system in southern Nevada, the measured $ET_r F$ between 10:30 to 11:00 was similar to the 24-hour average, so using the instantaneous $ET_r F$ as a proxy for the 24-hour average resulted in satisfactory daily ET estimates. For regionally expansive and water limited native vegetation,

the evaporative fraction (EF) approach is recommended over the $ET_r F$ approach to account for stomatal regulation, where EF equals the LE_{inst} divided by the available energy ($R_n - G$) [Bastiaanssen *et al.*, 1998]. For irrigated areas or well- irrigated riparian areas surrounded by arid environments the use of the ASCE-PM equation to estimate ET_r for time integration is recommended due to the ability of ET_r to capture the potential effects of advection (clothes line or oasis effect) on ET. Because this study focuses on agricultural areas surrounded by arid lands, the reference ET - crop coefficient approach ($ET_r * ET_r F$) in which ET_r is estimated with the ASCE-PM equation was applied for time integration of ET_{24i} for each study area. This approach has been shown to be accurate over a wide range of irrigated agricultural conditions [Kalma *et al.*, 2008; Gonzalez-Dugo *et al.*, 2009; Anderson *et al.*, 2012].

Time integration of ET_{24i} to the monthly and seasonal time scale is performed as:

$$ET = \sum_{i=n}^m ET_r F_i * ET_r_{24i}$$

where n and m are the first and last days of each month or season, respectively. In this study, n and m were specified to be the beginning and ending day of year for each month to develop monthly ET totals each year. Per-pixel linear interpolation of $ET_r F$ in-between satellite image dates was performed to estimate the daily value of $ET_r F$. Tasumi *et al.* [2005] and Liebert *et al.* [2015] show that this approach is effective for capturing changes due to growth stage, cuttings, harvests, and ultimately ET, however a minimum of one image per month is needed to capture these effects [Anderson *et al.*, 2012, 2015]. As expected, errors in daily ET estimates due to per-pixel time interpolation of $ET_r F$ generally decrease as the interval between satellite overpass decreases. Due to northwestern Nevada experiencing many cloud free day during the growing season, it is rare to have less than one unobscured image per month. The Mason Valley study area is located in the overlap area between Landsat path 43 and 42 (inset of Figure 1), and as a

result, cloud-free images with less than 8-day return times were especially frequent. The $ET_{r,24}$ used to multiply by the daily interpolated ET_rF was specific to each study area, and derived from local weather station data (Table 1) so that local conditions in each study area affecting ET_r and ultimately ET were considered. Figure 6 illustrates an example where daily ET_r is multiplied by time interpolated ET_rF to estimate daily ET for an alfalfa field in Mason Valley, where three alfalfa cuttings were observed.

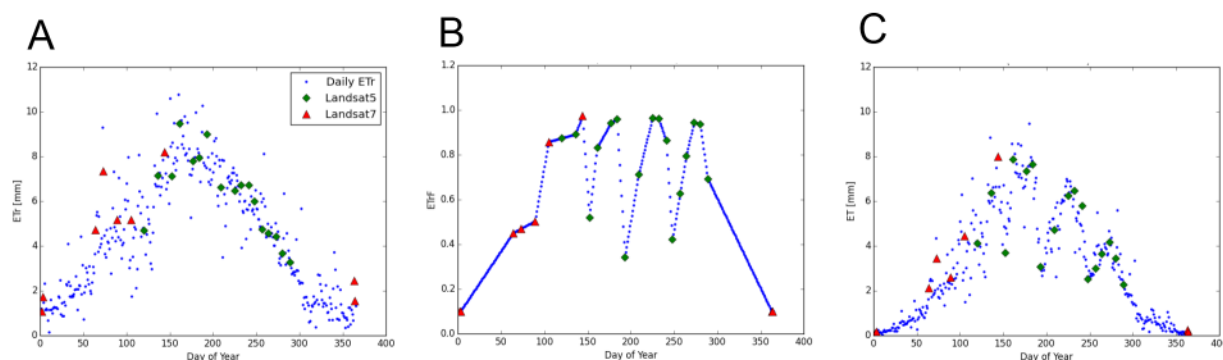


Figure 8 - Estimates of ET for a single agricultural field within Mason Valley, NV (2003) derived from (A) ET_r (B) ET_rF (C) ET .

Both early and late months of the calendar year are affected by a decrease in the number of usable Landsat images due to increased cloud cover, the interference of atmospheric inversions, and snow cover. In the report “Evapotranspiration and Net Irrigation Water Requirements for Nevada” (NVET), Huntington and Allen [2010] suggest that at an ET_rF of 0.1 to 0.2 typically reflects conditions of dormancy for agricultural vegetation. In order to provide estimates of early and late year ET , interpolations are anchored with an assumed ET_rF of 0.1 for the first day of the year and linearly interpolated to the ET_rF derived from the first usable Landsat image of the calendar year. Conversely, the ET_rF from the last usable Landsat image of the calendar year is linearly interpolated to the last day of the year, which is also assigned an ET_rF of 0.1.

In assigning an ET_rF of 0.1 for initial and final conditions, it is assumed that typical conditions are represented within the linear interpolation to the values before the first Landsat image, and conditions following the final useable Landsat image of the calendar year.

Application and Post Processing

Python programs outlined by Morton et al. [2013] were implemented to perform the METRIC process and time integration functions on multiple personal computers. The results were quality assured and controlled by evaluating statistics for each scene through calculation and visualization of ET_rF histograms, and calculation of the percentage of pixels above or below thresholds of 0.1 and 1.05, respectively. Large populations of pixels outside these extremes were cause for the re-calibration of METRIC through the re-selection of hot and cold pixel locations, and the re-running of METRIC until a reasonable distribution of ET_rF was obtained. This iterative approach is similar to what is employed during automated calibration of METRIC [Morton et al., 2013]. Once satisfactory results were obtained, per-pixel monthly and seasonal ET aggregations were made from 2001 and 2011. Per-pixel monthly and seasonal ET estimates were then averaged spatially, using digitized field polygon boundaries (Figure 7) to develop average monthly and seasonal ET totals for agricultural areas within each study area. Basin ET totals were calculated as the sum of the area weighted average of all agricultural areas within the basin, divided by the total area. Monthly precipitation estimates derived from PRISM were used to estimate spatially averaged monthly and seasonal net ET for each study area.

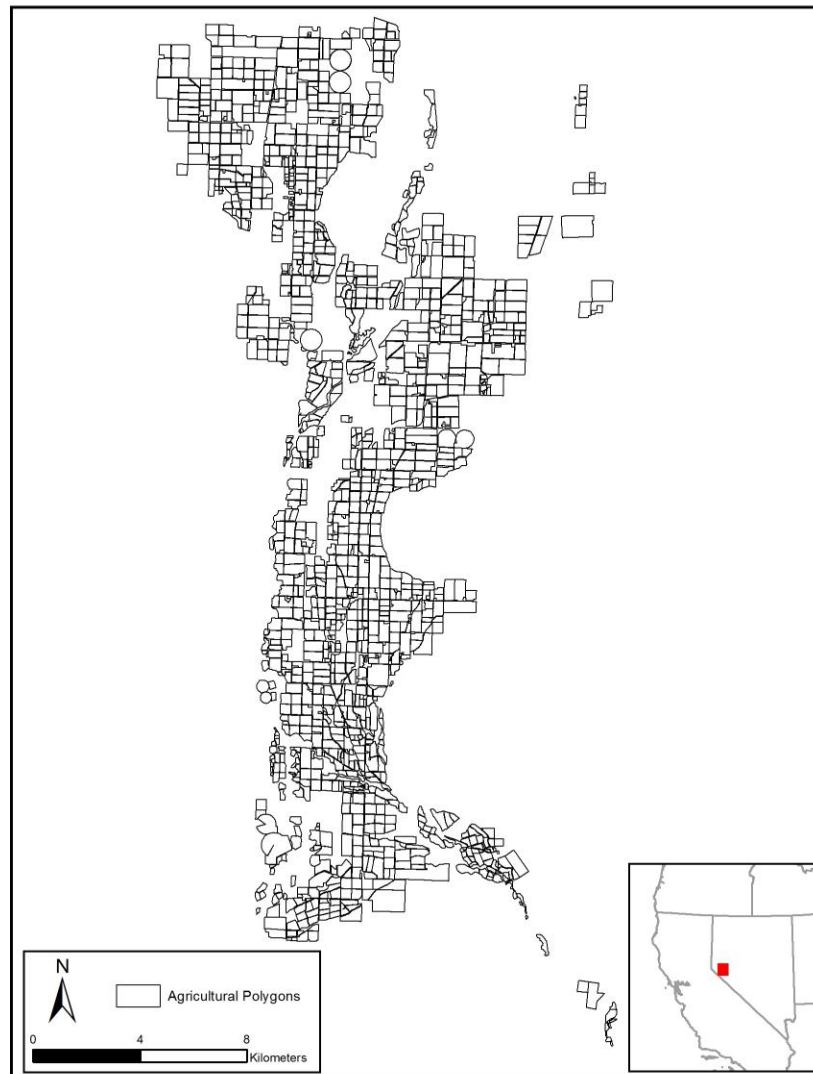


Figure 9 – Example of agricultural polygons adapted from CLU data, used to spatially aggregate ET calculations (Mason Valley, NV)

Results

To compare and contrast the effects of drought, resiliency in water source, and changes associated with water rights transfers, area weighted averages of annual, seasonal, and monthly

ET were aggregated for each study area. Annual and seasonal ET rates ranged from 1282 to 309 mm, and 1070 to 241 mm, respectively, across all study areas. Variability of annual ET and annual net ET was much higher for Lovelock and Fish Springs Ranch than in Fallon and Mason Valley (Figures 10A, 10C).

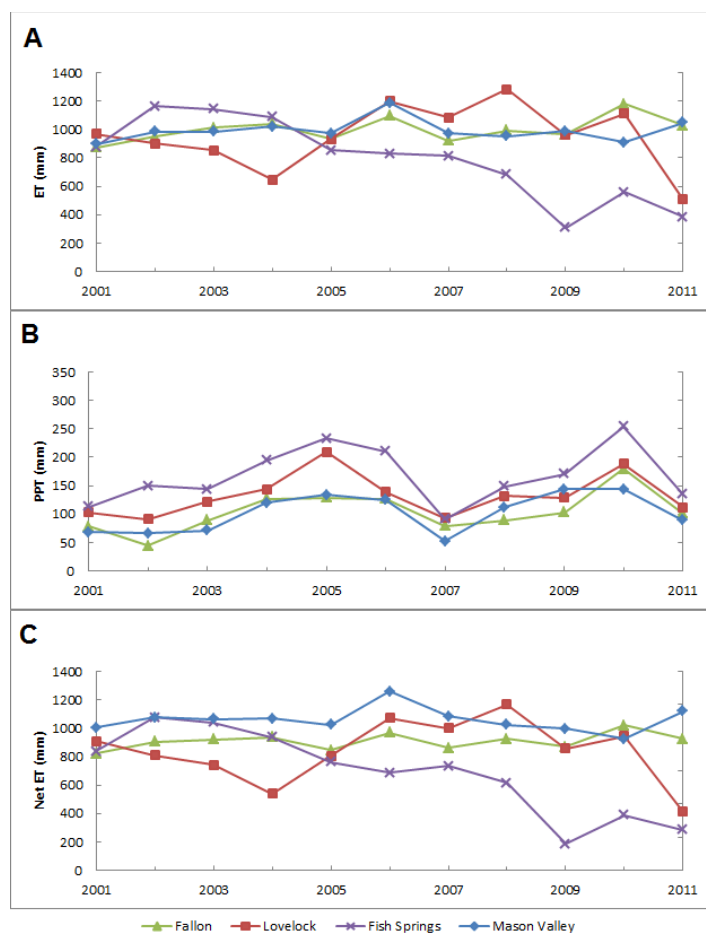


Figure 10 - (A) Annual ET, (B) Annual precipitation, (C) Annual net ET for each study area, during the period of study.

In comparing the annual ET for the study areas, Fallon exhibited the highest mean annual ET and mean net ET, with Mason Valley exhibiting similar values. Fish Springs Ranch demonstrated the lowest annual mean ET and annual mean net ET over the study period (Figure 10).

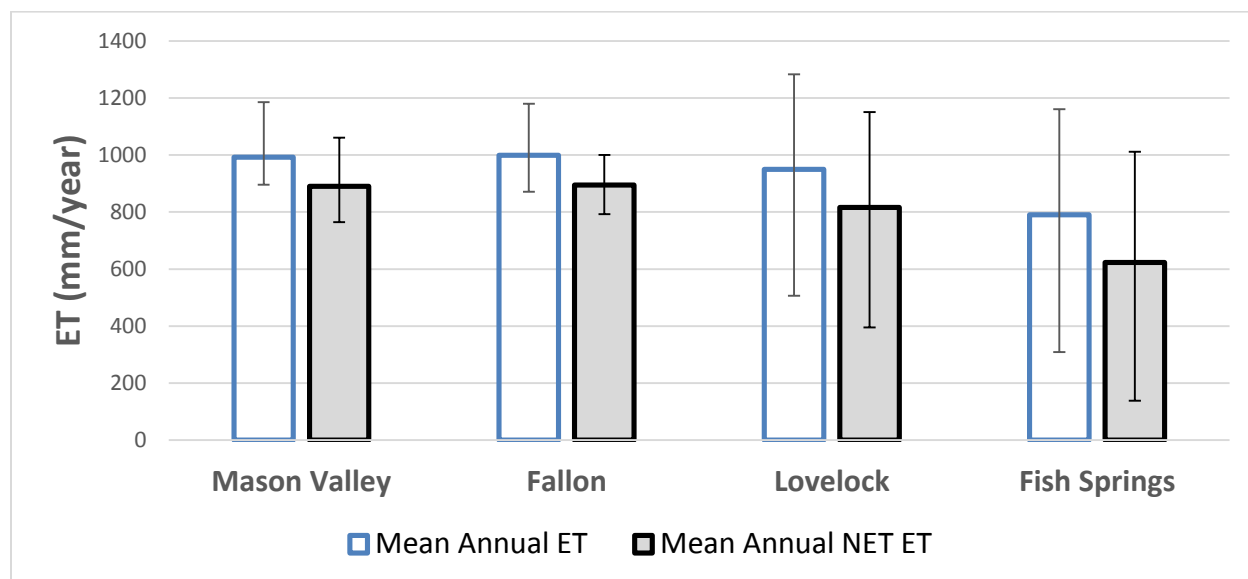


Figure 11- Mean annual ET and annual net ET for each area of study. Upper and lower bars illustrate respective maxima and minima for each study area.

These results are similar to calculations of mean seasonal ET and mean seasonal net ET (Figure 9), in that Lovelock had the highest mean seasonal ET and mean seasonal net ET, followed by Fallon, with Fish Springs Ranch exhibiting the lowest mean seasonal ET and mean seasonal net ET over the study period. The maximums for each study area diverged from the mean, in that Lovelock exhibited the highest maximum seasonal ET and seasonal net ET.

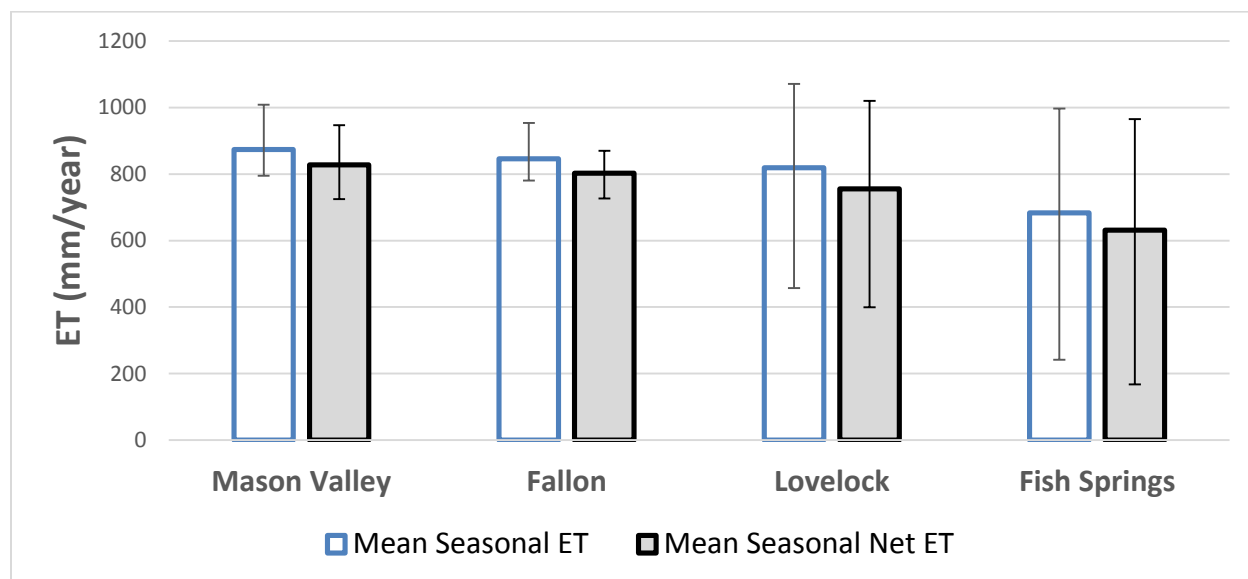


Figure 12 - Mean seasonal ET and seasonal net ET for each area of study. Upper and lower bars illustrate respective maxima and minima for each study area.

Total ET for each month was used to create matrix plots, which illustrated ET for each study area during the period of study (Figure 13). These plots exposed patterns and trends in annual and seasonal ET. The figures of ET used to create the matrix plots are located in the appendix of this document.

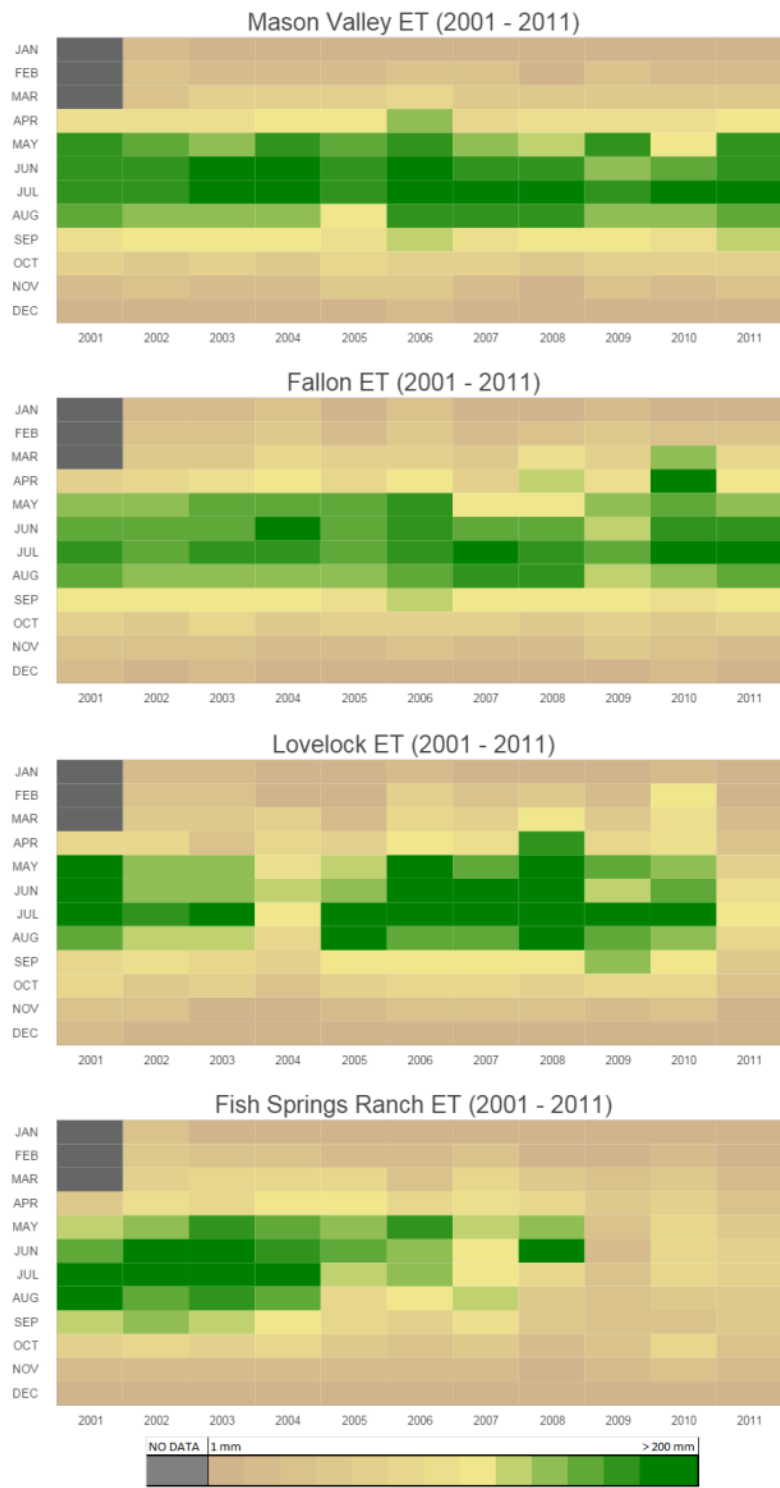


Figure 13 – Variation in ET across months and years for Mason Valley, Fallon, Lovelock, and Fish Springs Ranch.

In Mason Valley, each year begins with minimal ET due to low ET_r , followed by an increase in ET during the crop development stage, with ET reaching a maximum during June and July during full canopy cover and maximum ET_r . ET declines sharply in September and remains at minimal levels until March and April the following spring. This seasonal pattern of ET reflects the normal progression of initial development, maturity, and dormancy crop stages for a well-irrigated agricultural environment, and is strongly connected to annual patterns of ET_r . This yearly cycle is relatively consistent for Mason Valley, even through periods of drought that occurred during 2001-2003 and 2009-2010 (Figure 13). The decrease in seasonal ET associated with limitations in surface water supply can be seen best in comparing the geographic distribution of seasonal ET for a year that was exceptionally dry and the seasonal distribution of ET for a year that received ample deliveries of surface water (Figure 14). In years of limited surface water, areas of high ET were concentrated in areas where supplemental groundwater pumping is used to compensate for deficits in surface water.

The matrix plot for Fallon illustrates monthly and seasonal ET patterns that are similar to Mason Valley; however, the study area experienced a noticeable drop in ET during 2009, coinciding with a period of drought (Figure 13). The spatial distribution of seasonal ET during the wettest year and driest year for the Fallon study area did not reveal any obvious patterns (Figure 15).

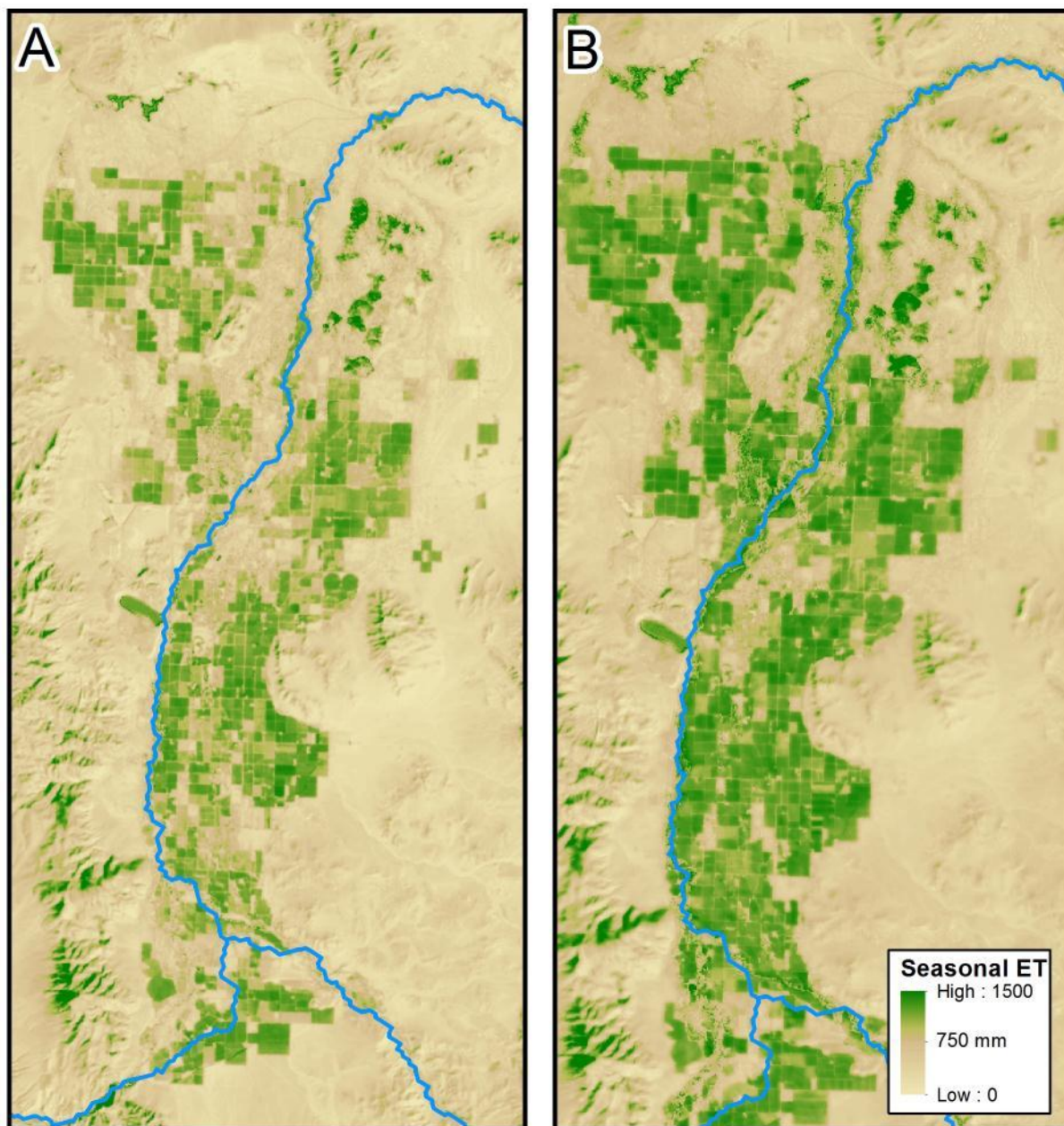


Figure 14 - Comparison of seasonal ET in Mason Valley for (A) 2002, in which the area received below average precipitation and surface water deliveries, and (B) 2006, which was not restricted by water.

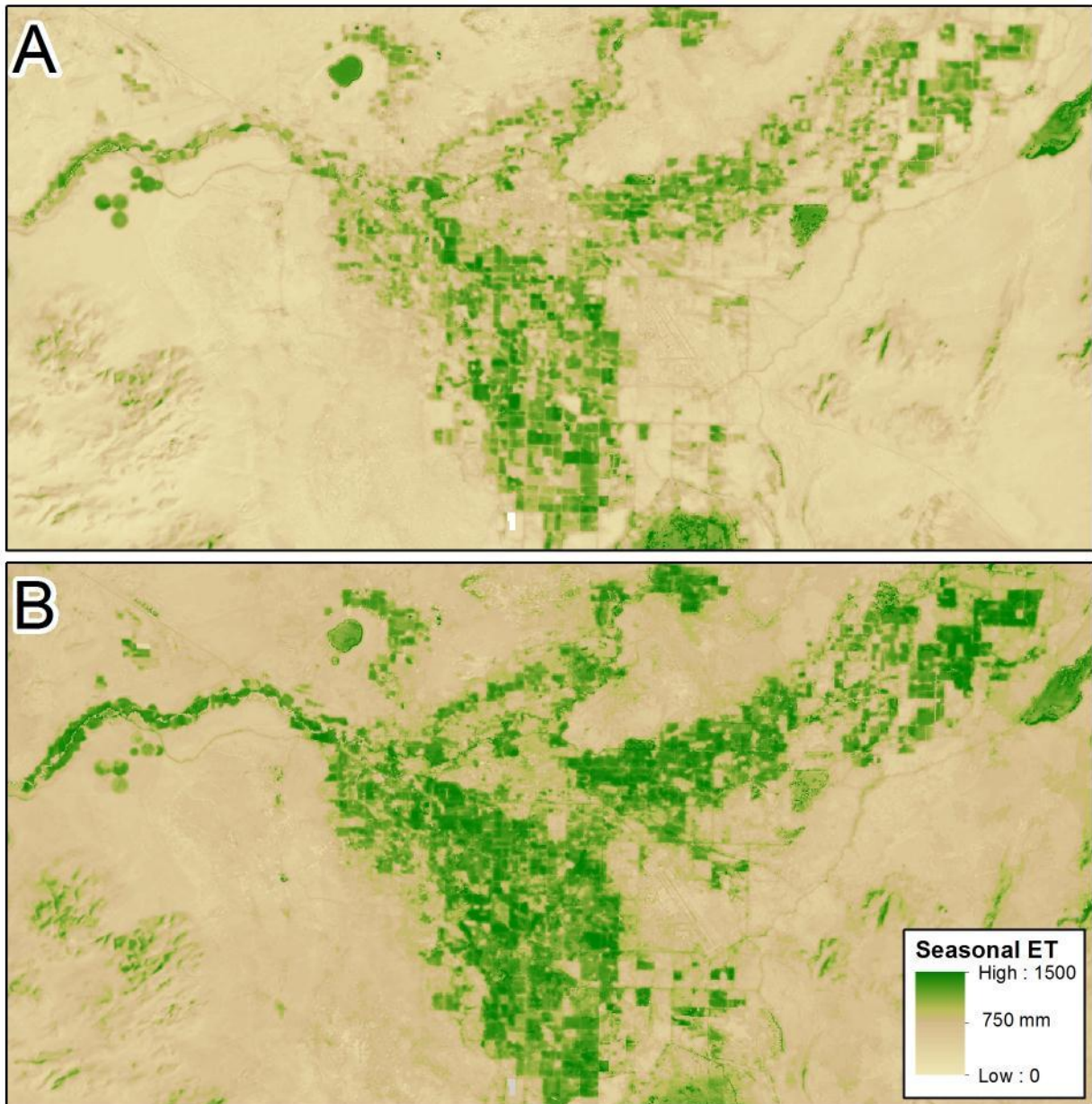


Figure 15 - Comparison of seasonal ET for Fallon, NV for (A) 2009, in which the area received below average precipitation and surface water deliveries, and (B) 2010, which was not restricted by water.

Monthly ET results for Lovelock illustrate large annual and seasonal variability, where ET is greatly reduced during periods of extended drought (Figure 13). Limited access to surface water reduced agricultural areas to near-background rates of ET during 2004, compared with a 2006, which was not limited in the supply of surface water (Figure 16).

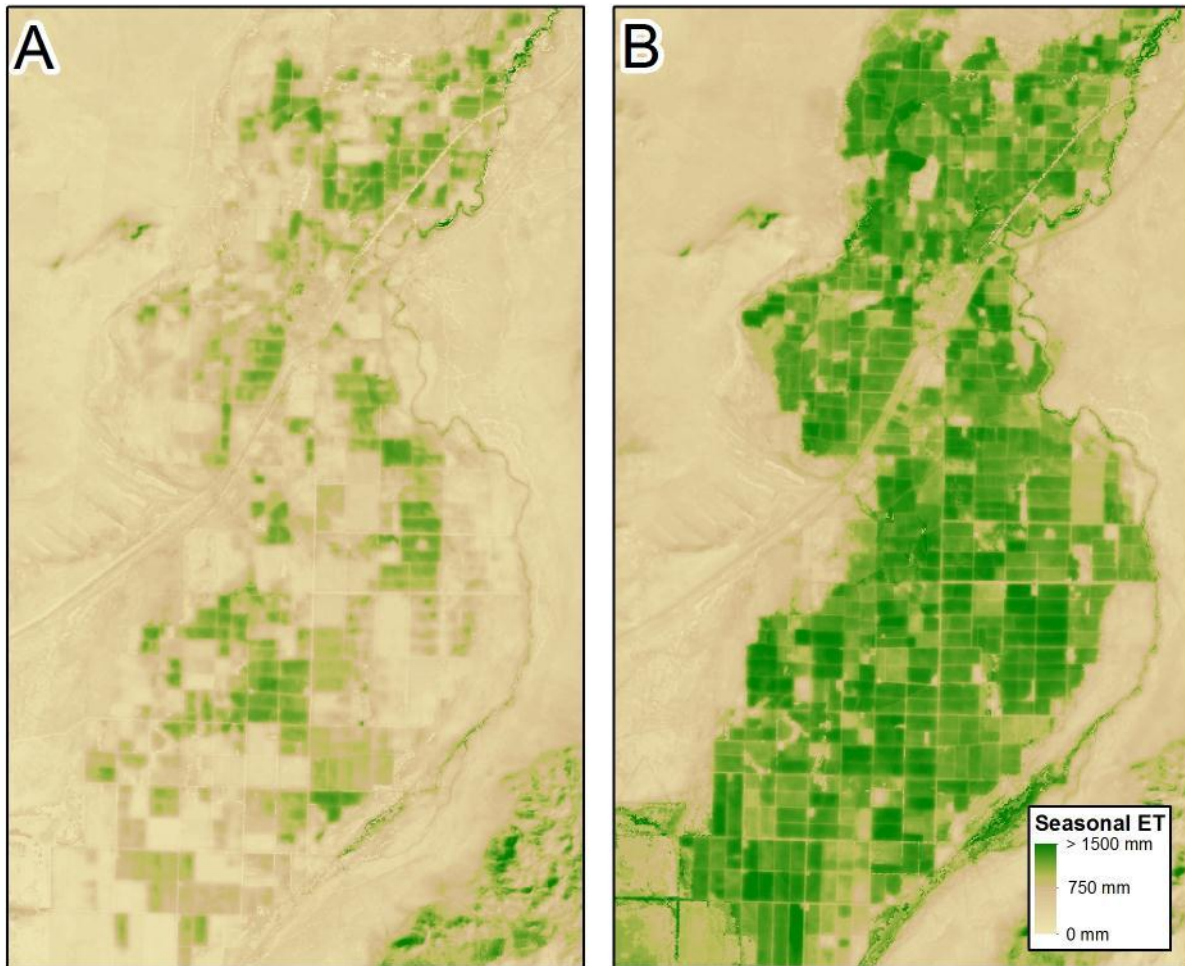


Figure 16 - Comparison of ET for Lovelock, NV. (A) 2004 represents a period affected by an occurrence of multi-year drought, while (B) 2006 is provided adequate water, due to the replenishment of water resources.

Fish Springs Ranch exhibited consistent seasonal ET until it sharply declined in 2005, with even further declines evident in 2009 (Figure 15). Examples of the spatial distribution of seasonal ET for selected study areas are shown in Figures 13-15 to provide a spatial context to ET calculations illustrated in the matrix plots.

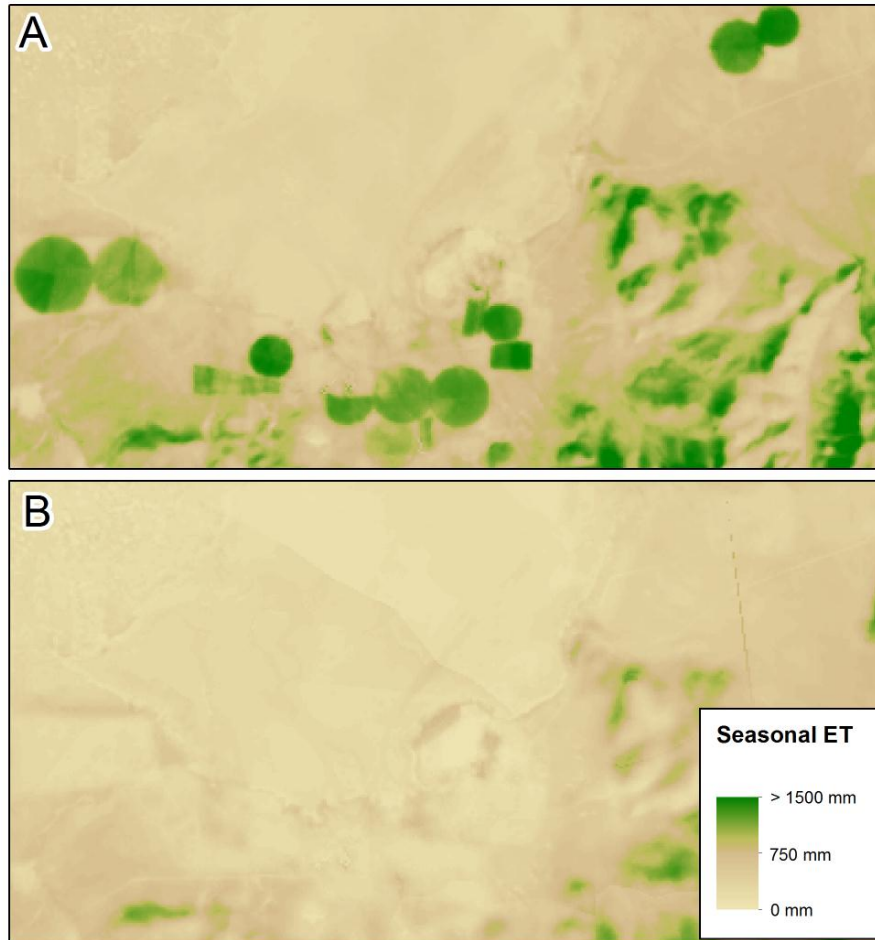


Figure 17 - Comparison of ET for Fish Springs Ranch for (A) 2002, while irrigation was conducted and (B) 2009, after groundwater rights were converted to municipal use and irrigation ceased.

Discussion

The estimates of ET derived from this energy balance approach reveal significant patterns in water consumption, which relate to drivers of agricultural water consumption. Actual ET is observed as being significantly lower than potential crop ET due to water limitations, stress, farming practice (i.e. harvests, crop rotations, fallowing), and land use change connected to the transfer of water. The susceptibility and the resilience demonstrated by the study areas are clearly seen in the results illustrated in Figures 13.

The first question asked in this work was answered in that wet years were observed as having high ET, conversely dry years and years afflicted by multi-year drought expressed significantly depressed ET. Even with ample upstream storage on the Truckee and Carson River systems, some drought events, such as that occurring in 2009, reduced surface water diversions from Lahontan Reservoir (Figure 19). This decrease in the delivery of water resulted in suppressed ET for the Fallon study area.

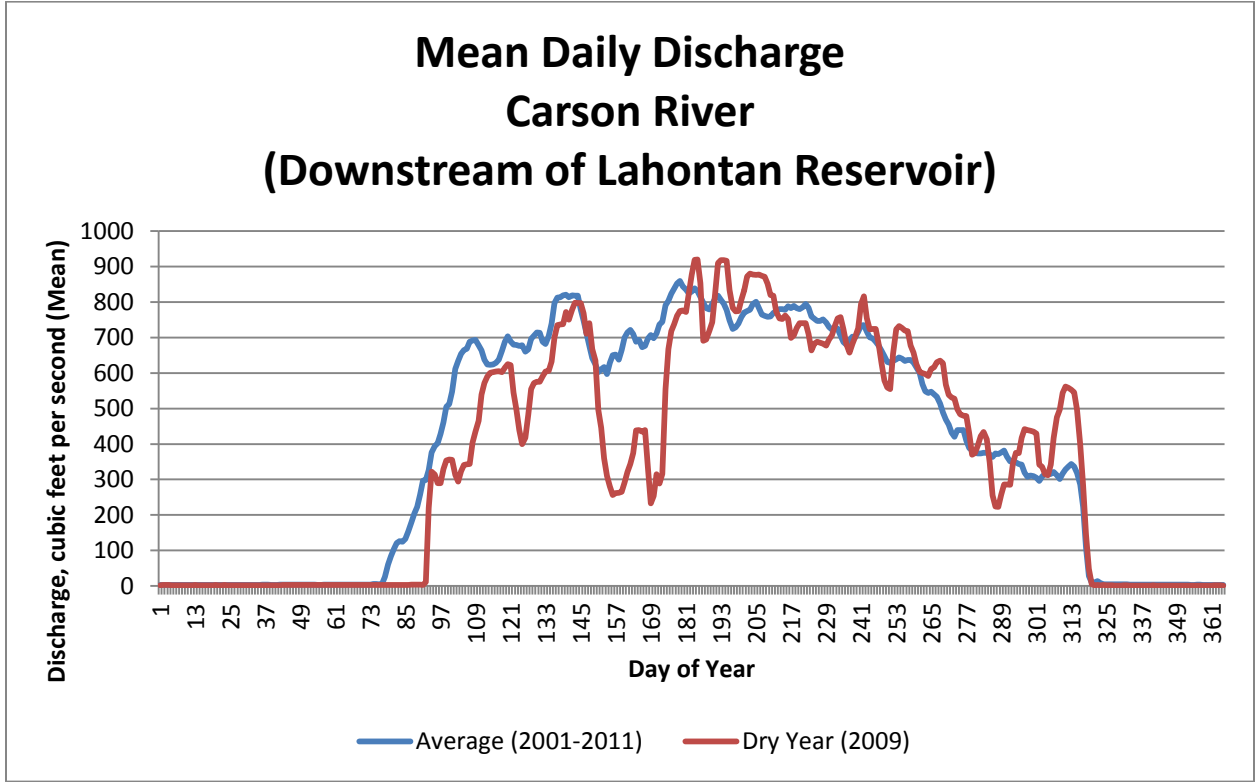


Figure 18 - Comparison of mean daily flows of the Carson River (USGS 10312150 CARSON RV BLW LAHONTAN RESERVOIR NR FALLON, NV).

During times of drought, irrigation in Lovelock was reduced and even completely cut off due to the lack of water. The impact of reduced irrigation on ET is evident during the drought of the early 2000s, increasing with severity from 2001-2004 (Figure 20).

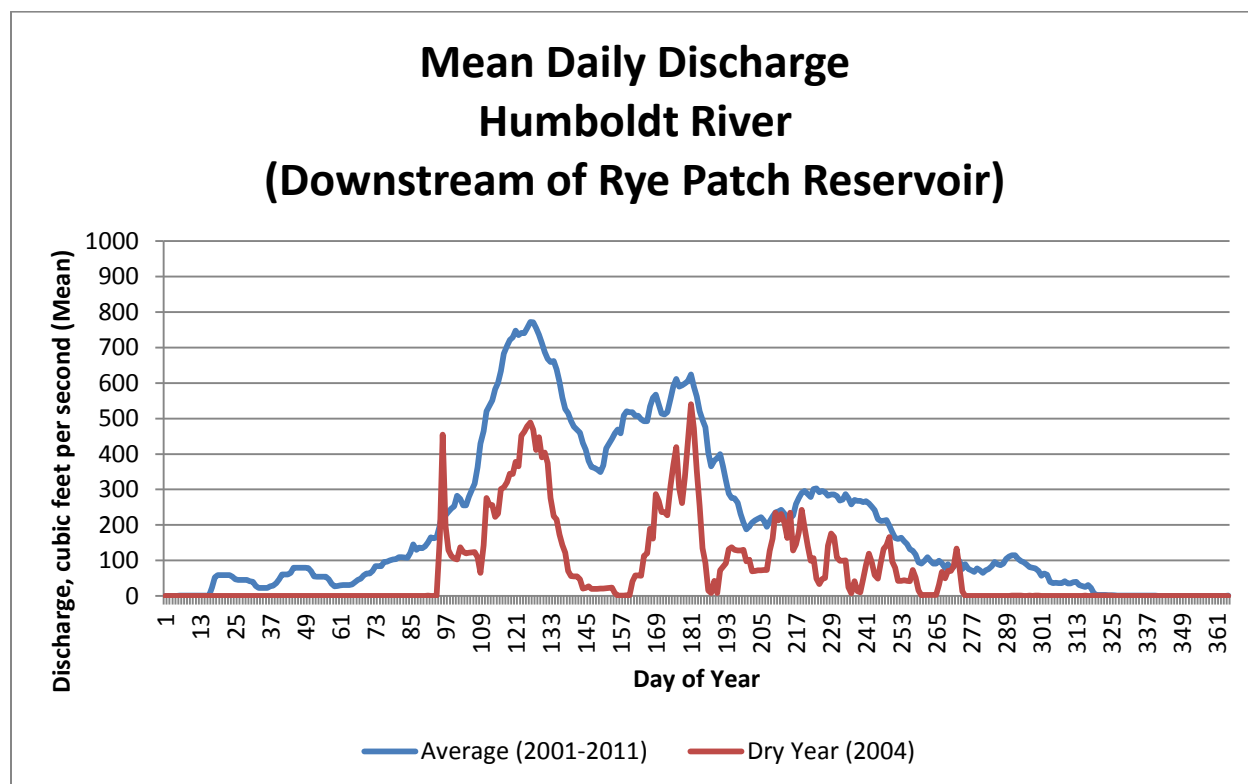


Figure 19 - Comparison of mean daily flows of the Humboldt River (USGS 10335000 HUMBOLDT RV NR RYE PATCH, NV).

The drought of the early 2000's concluded in 2005, when the drought broke and precipitation replenished the supply of water stored in Rye Patch Reservoir. Another period of drought occurred from 2009 through 2011, corresponding to a second period of decreased ET for the Lovelock study area (Figure 13).

The second questions was answered in that annual patterns of ET were more stable for Mason Valley and Fallon due to these areas receiving water from more than one source. Mason Valley receives water primarily from surface water diversions of the Walker River, with significant supplemental groundwater pumping during periods of drought and low river flows. Fallon is also well buffered from periods of drought due to ample upstream storage on both the Truckee

River and Carson River systems. This diversity in surface water sources compensates for the lack of access to groundwater suitable for agriculture.

The stable and persistent seasonal ET pattern exhibited in Mason Valley and Fallon is in stark contrast to the results of Lovelock and Fish Springs Ranch. Lovelock conducts irrigation with water from a single surface water source (Humboldt River) and benefits from only a limited amount of upstream storage within Rye Patch Reservoir. Because of the reliance on surface water from the Humboldt River, lack of upstream storage, and the inability to utilize groundwater for irrigation, Lovelock is extremely susceptible to droughts of various intensity and duration.

In contrast to the impacts of weather and water source on ET observed in Mason Valley, Fallon, and Lovelock, the third question was addressed by examining ET for Fish Springs Ranch in the context of the transfer of water and the associated land-use change (Figure 15). In 2000, Fish Springs Ranch was acquired by Vidler Water Company in order to procure 13,000 acre-feet of groundwater rights associated with the property [*Vidler Water Company, 2015*]. A change in the manner of use, from irrigation to municipal, and an inter-basin transfer from the Honey Lake Basin to Lemmon Valley was granted by the Nevada State Engineer. Vidler continued to operate the ranch with limited irrigation until 2007, when water works were installed to transfer pumped groundwater into Lemmon Valley via a pipeline (Figure 1). After 2007, ET rates reduced to natural background levels due to the fallowing of agricultural lands.

Annual ET results during years with ample water supply compare well with previous estimates of crop ET in each study area. Huntington and Allen [2010] estimated crop ET under well-irrigated and stress free conditions for 256 hydrographic areas in Nevada using local climate

data, crop type information, and a daily crop ET and soil water balance model for Evapotranspiration and Net Irrigation Water Requirements for Nevada (NVET). While a comparison of ET to respective years was not possible due to non-overlapping study periods, comparing mean annual alfalfa ET estimates from NVET to mean annual ET estimates from this study provides useful information in distinguishing differences between the actual crop consumptive use and the potential consumptive use under well- irrigated conditions. NVET reported mean annual alfalfa ET to be 1067 mm, 1097 mm, 1250 mm, and 1158 mm for Mason Valley, Fallon, Lovelock, and Fish Springs Ranch, respectively. These estimates are similar to maximum annual ET estimates from this study of 1185mm, 1180mm, 1282mm, and 1161mm, for Mason Valley, Fallon, Lovelock, and Fish Springs Ranch, respectively (Table 2, Figure 18).

Table 3 - Comparison of NVET estimates, with calculated ET from this study

Study Area	Mean Annual Alfalfa ET - (Huntington and Allen, 2010) (mm)	Maximum Annual ET - This Study (mm)	Mean Annual ET - This Study (mm)	Minimum Annual ET - This Study (mm)
Mason Valley	1067	1185	992	1067
Fallon	1097	1180	999	1097
Lovelock	1250	1282	949	1250
Fish Springs Ranch	1158	1161	791	1158

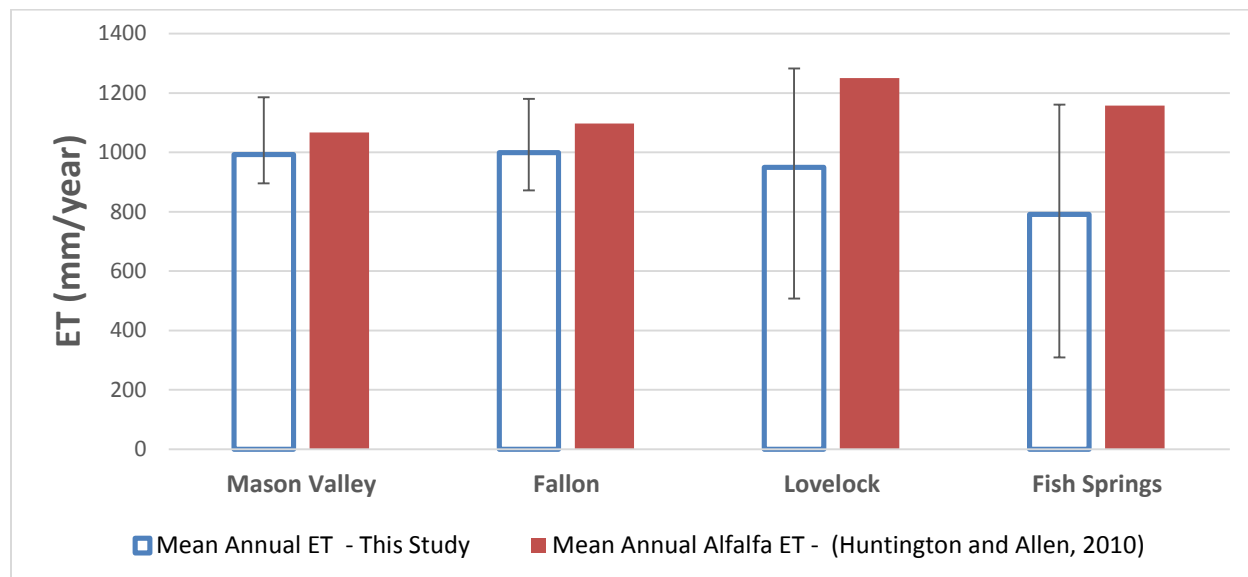


Figure 20 - ET estimates from this study are compared to estimates by NVET (Huntington and Allen, 2010). Maximum and minimum rates of annual ET are represented with upper and lower bars.

Differences between the estimated maximum annual ET reported in this study versus the respective mean annual alfalfa ET estimate reported by Huntington and Allen in NVET [2010] are likely due to inaccuracies and differences in the modeling approaches, differences in crop types, and differences in the time periods compared. Given that the majority of crop acreage grown within the study areas is alfalfa, it makes sense that the alfalfa ET estimates in NVET compare well with maximum annual ET rates reported in this study. This is especially true for Lovelock and Fish Springs Ranch, where alfalfa comprises nearly all of the crop acreage, and the comparison of maximum annual ET from this study compares best with Huntington and Allen [2010]. Of interest is the large difference between the mean annual ET reported in NVET and the mean annual ET derived from METRIC in this work. This difference is effectively the difference between the potential consumptive use and the actual consumptive use due to water limitations. Identifying the actual crop consumptive use is especially important for monitoring actual water use and developing water budgets, and only historical satellite imagery can provide such estimates over large regions and long histories.

Methods applied for estimating ET in this work are subject to uncertainties and limitations. Uncertainties and limitations with ET methods applied in this study are the result of errors in model structure, inaccuracies in instrumentation used to collect meteorological data, inaccuracies in estimated weather data from METDATA, and inaccuracies in Landsat satellite information. However, models used in this study have been shown to result in fairly accurate ET estimates in Nevada [*Morton et al.*, 2013; *Liebert et al.*, 2015].

Conclusions

The primary objective of this study was to explore patterns of water consumption for four contrasting agricultural communities within northwestern Nevada. I found a strong positive relationship between ET and the amount of water available to agriculture, directly from precipitation and through the diversion of surface-water which originates from yearly precipitation. I found that variations in ET during wet and dry years was less pronounced depending on whether the study area has access to multiple sources of water or can buffer changes in water availability with the storage of water. I found that where water was repurposed from agricultural to municipal use, ET dropped to background levels.

Water consumption from agricultural areas was examined through remotely sensed ET estimates using a land surface energy balance model, METRIC. The influence of weather was both significant and detectable as the effects of multi-year droughts were seen in seasonal and annual patterns of ET, mostly in Lovelock. Despite being exposed to similar variations in precipitation, Fallon and Mason Valley exhibited the least amount of variability in water consumption due to

the utilization of multiple and diverse sources of water. The change in the manner of water use from irrigation to municipal, and exportation of water from Fish Springs Ranch was evident in both seasonal and annual patterns of ET, as the irrigation of agricultural land was ceased.

Remotely sensed land surface energy balance modeling of actual ET captures the effects of land management, water management, and climatic influences. ET estimates produced in this study have many immediate applications relevant to the water and environmental science communities, and decision makers. Additionally, analyzing ET over long time histories and with respect to environmental and land use change, is an effective way to assess potential future impacts of drought, changing water source, and land use change in agricultural communities.

The approach outline in this work has implications outside of northwestern Nevada, as water managers work to address the problems of scarcity. An adage used in business states: "You can't manage what you can't measure." This paradigm has implications for the challenges of resource management. ET estimates developed through an energy balance approach provide high-resolution data at an unprecedented scale. Gaining information on the past usage of water in the context of drivers and limiting factors will help us better plan and adapt for the future.

Bibliography

- Abatzoglou, J. T. (2013), Development of gridded surface meteorological data for ecological applications and modelling, *Int. J. Climatol.*, 33(1), 121–131.
- Allen, R. (2008), Quality Assessment of Weather Data and Micrometeorological Flux-Impacts on Evapotranspiration Calculation, *農業気象 (Journal Agric. Meteorol.)*, 64(4), 191–204, doi:10.2480/agrmet.64.4.5.
- Allen, R. G. (1996), Assessing integrity of weather data for reference evapotranspiration estimation, *J. Irrig. Drain. Eng.*, 122(2), 97–106.

- Allen, R. G. (2011), Ref-ET: Reference Evapotranspiration Calculator - Version - Windows 3.1.10. University of Idaho, Available from: <http://extension.uidaho.edu/kimberly/2013/04/ref-et-reference-evapotranspiration-calculator/> (Accessed 17 April 2015)
- Allen, R. G., C. E. Brockway, and J. L. Wright (1983), Weather station siting and consumptive use estimates, *J. Water Resour. Plan. Manag.*, 109(2), 134–136.
- Allen, R. G., L. S. Pereira, D. Raes, and M. Smith (1998a), *Crop evapotranspiration (guidelines for computing crop water requirements)*.
- Allen, R. G., L. S. Pereira, D. Raes, M. Smith, and others (1998b), Crop evapotranspiration—Guidelines for computing crop water requirements—FAO Irrigation and drainage paper 56, *FAO, Rome, 300(9)*, D05109.
- Allen, R. G., I. A. Walter, R. Elliot, and T. A. Howell (2005), ASCE-EWRI Standardization of Reference Evapotranspiration, *Am. Soc. Civ. Eng. Water Inst.*
- Allen, R. G., M. Tasumi, and R. Trezza (2007), Satellite-Based Energy Balance for Mapping Evapotranspiration with Internalized Calibration (METRIC)—Model, *J. Irrig. Drain. Eng.*, 133(4), 380–394, doi:10.1061/(ASCE)0733-9437(2007)133:4(380).
- Allen, R. G., L. S. Pereira, T. a. Howell, and M. E. Jensen (2011), Evapotranspiration information reporting: I. Factors governing measurement accuracy, *Agric. Water Manag.*, 98(6), 899–920, doi:10.1016/j.agwat.2010.12.015.
- Allen, R. G., R. Trezza, M. Tasumi, and J. Kjaersgaard (2014), METRIC applications manual for Landsat satellite imagery, Version 3.0, *Univ Idaho, Kimberly*.
- Anderson, M. C., R. G. Allen, A. Morse, and W. P. Kustas (2012), Use of Landsat thermal imagery in monitoring evapotranspiration and managing water resources, *Remote Sens. Environ.*, 122, 50–65, doi:10.1016/j.rse.2011.08.025.
- Anderson, M. C., K. A. Semmens, F. Gao, C. Hain, W. P. Kustas, J. G. Al, J. H. Prueger, L. Mckee, and W. Dulaney (2015), Monitoring Daily Evapotranspiration at Field- to-Regional Scales : An Application over California Vineyards using Landsat 8, *Remote Sens. Environ.*, 2014–2016.
- Barros, V. R. et al. (2014), *Climate Change 2014: Impacts, Adaptation, and Vulnerability. Part B: Regional Aspects. Contribution of Working Group II to the Fifth Assessment Report of the Intergovernmental Panel on Climate Change*, Cambridge University Press, Cambridge.
- Bastiaanssen, W. G. M., M. Menenti, R. A. Feddes, and A. A. M. Holtslag (1998), A remote sensing surface energy balance algorithm for land (SEBAL). 1. Formulation, *J. Hydrol.*, 212–213, 198–212, doi:10.1016/S0022-1694(98)00253-4.

- Berris, S., G. Hess, and L. Bohman (2001), *River and Reservoir Operations Model, Truckee River Basin, California and Nevada, 1998*.
- Bos, M. G., R. AL Kselik, R. G. Allen, and D. Molden (2009), Water Requirements for Irrigation and the Environment, , 174, doi:10.1007/978-1-4020-8948-0.
- Cammalleri, C., M. C. Anderson, and W. P. Kustas (2014), Upscaling of evapotranspiration fluxes from instantaneous to daytime scales for thermal remote sensing applications, *Hydrol. Earth Syst. Sci.*, 18(5), 1885–1894, doi:10.5194/hess-18-1885-2014.
- Carroll, R. W. H., G. Pohll, D. McGraw, C. Garner, A. Knust, D. Boyle, T. Minor, S. Bassett, and K. Pohlmann (2010), Mason Valley Groundwater Model: Linking Surface Water and Groundwater in the Walker River Basin, Nevada, *JAWRA J. Am. Water Resour. Assoc.*, doi:10.1111/j.1752-1688.2010.00434.x.
- Chander, G., and B. Markham (2003), Revised landsat-5 tm radiometric calibration procedures and postcalibration dynamic ranges, *IEEE Trans. Geosci. Remote Sens.*, 41(11), 2674–2677, doi:10.1109/TGRS.2003.818464.
- Collatz, G. J., J. T. Ball, C. Grivet, and J. A. Berry (1991), Physiological and environmental regulation of stomatal conductance, photosynthesis and transpiration: a model that includes a laminar boundary layer, *Agric. For. Meteorol.*, 54(2-4), 107–136, doi:10.1016/0168-1923(91)90002-8.
- Daly, C., W. Gibson, and G. Taylor (2002), A knowledge-based approach to the statistical mapping of climate, *Clim.*
- DeLong, J. (2015), Pipeline would provide new water for North Valleys, *Reno Gazette-Journal*, 29th April.
- Dingman, S. L. (2008), *PHYSICAL HYDROLOGY*, Second Edi., Waveland Press.
- Everett, D. E., and F. E. Rush (1965), *Water Resources Appraisal of Lovelock Valley, Pershing County, Nevada*, State of Nevada Department of Conservation and Natural Resources.
- Fry, J. a. J., G. Xian, S. Jin, J. a. J. Dewitz, C. G. Homer, L. Yang, C. a. Barnes, N. D. Herold, and J. D. Wickham (2011), Completion of the 2006 national land cover database for the conterminous United States, *Photogramm. Eng. Remote Sensing*, 77(9), 858–864.
- Gonzalez-Dugo, M. P., C. M. U. Neale, L. Mateos, W. P. Kustas, J. H. Prueger, M. C. Anderson, and F. Li (2009), A comparison of operational remote sensing-based models for estimating crop evapotranspiration, *Agric. For. Meteorol.*, 149(11), 1843–1853, doi:10.1016/j.agrformet.2009.06.012.
- Guitjens, J. C., and M. T. Goodrich (1994), Dormancy and nondormancy alfalfa yield and evapotranspiration, *J. Irrig. Drain. Eng.*, 120(6), 1140–1146.

- Hendrickx, J. M. H. (2010), *ET Mapping in the Green River Basin - Second Stage, Growing Season.*, Final Report to the University of Wyoming. Soil Hydrology Associates, LLC.,
- Hobbins, M. T., and J. Huntington (2015), *Chapter 44: Evapotranspiration and evaporative demand. Submitted to Handbook of Applied Hydrology*, McGraw-Hill Publishing.
- Hoffman, R. J., R. J. Hallock, T. G. Rowe, M. S. Lico, H. L. Burge, and S. P. Thompson (1990), *Reconnaissance investigation of water quality, bottom sediment, and biota associated with irrigation drainage in and near Stillwater Wildlife Management Area, Churchill County, Nevada, 1986-87*, Department of the Interior, US Geological Survey.
- Homer, C., J. Dewitz, J. Fry, M. Coan, N. Hossain, C. Larson, N. Herold, A. McKerrow, J. N. VanDriel, and J. Wickham (2007), Completion of the 2001 National Land Cover Database for the Conterminous United States, *Photogramm. Eng. Remote Sensing*, 73(4), 337–341, doi:citeulike-article-id:4035881.
- Homer, C. G., J. A. Dewitz, L. Yang, S. Jin, P. Danielson, G. Xian, J. Coulston, N. D. Herold, J. D. Wickham, and K. Megown (2015), Completion of the 2011 National Land Cover Database for the conterminous United States-Representing a decade of land cover change information, *Photogramm. Eng. Remote Sensing*, 81(5), 345–354.
- Hunsaker, D. J., J. P. J. Pinter, E. M. Barnes, and B. A. Kimball (2003), Estimating cotton evapotranspiration crop coefficients with a multispectral vegetation index, *Irrig. Sci.*, 22(2), 95–104, doi:10.1007/s00271-003-0074-6.
- Huntington, J. L., and R. G. Allen (2010), *Evapotranspiration and Net Irrigation Water Requirements for Nevada*, pp. 1–15, American Society of Civil Engineers, Carson City, Nevada.
- Huntington, J. L., C. G. Morton, M. Bromley, R. Liebert, and K. Paudel (2014), *Landsat Evapotranspiration from Phreatophyte and Irrigated Areas, Boulder Flat, Humboldt River Basin, Nevada*, Desert Research Institute.
- Huntington, J. L., S. Gangopadhyay, J. M. Spears, R. G. Allen, C. King, C. G. Morton, A. Harrison, D. McEvoy, and A. Joros (2015), *West-wide climate risk assessments: Bias-corrected and spatially downscaled irrigation demand and reservoir evaporation projections. U.S. Bureau of Reclamation*, US Department of the Interior, Bureau of Reclamation, Technical Service Center.
- Kalma, J., T. McVicar, and M. McCabe (2008), Estimating Land Surface Evaporation: A Review of Methods Using Remotely Sensed Surface Temperature Data, *Surv Geophys*, 29(4-5), 421–469.
- Katerji, N., J. W. Van Hoorn, A. Hamdy, M. Mastrorilli, and F. Karam (1998), Salinity and

- drought, a comparison of their effects on the relationship between yield and evapotranspiration, *Agric. Water Manag.*, 36(1), 45–54.
- Kjaersgaard, J., and R. G. Allen (2010), *Remote Sensing Technology to Produce Consumptive Water Use Maps for the Nebraska Panhandle*.
- Liebert, R., J. Huntington, C. Morton, S. Sueki, and K. Acharya (2015), Reduced evapotranspiration from leaf beetle induced tamarisk defoliation in the Lower Virgin River using satellite based energy balance, *Ecohydrology*, doi:10.1002/eco.1623.
- McNaughton, K. G., and P. G. Jarvis (1991), Effects of spatial scale on stomatal control of transpiration, *Agric. For. Meteorol.*, 54(2-4), 279–302, doi:10.1016/0168-1923(91)90010-N.
- Mitchell, K. E. et al. (2004), The multi-institution North American Land Data Assimilation System (NLDAS): Utilizing multiple GCIP products and partners in a continental distributed hydrological modeling system, *J. Geophys. Res.*, 109(D7), D07S90–, doi:10.1029/2003JD003823.
- Morton, C. ., J.L. Huntington, A. Joros, R.G. Allen, and A. Kilic (2015a), More Landsat Satellites Equates to More Reliable Monitoring of Water Consumption., *Submitt. to J. Remote Sensing*.
- Morton, C. G., J. L. Huntington, G. M. Pohl, R. G. Allen, K. C. Mcgwire, and S. D. Bassett (2013), Assessing Calibration Uncertainty and Automation for Estimating Evapotranspiration from Agricultural Areas Using METRIC, *J. Am. Water Resour. Assoc.*, 49(3), 549–562, doi:10.1111/jawr.12054.
- Morton, C. G., J. L. Huntington, F. Melton, A. Guzman, and R. Allen (2015b), Implementation of Automated METRIC Algorithms on the NASA Earth Exchange for Rapid Consumptive Water Use and Drought Impact Mapping in California’s Central Valley.,
- Nevada Department of Agriculture (2015), Agriculture in Nevada, Available from: http://agri.nv.gov/Administration/Administration/Agriculture_in_Nevada/
- NRCS (2015), Description of SSURGO Database | NRCS, *Descr. SSURGO Database*. Available from: http://www.nrcs.usda.gov/wps/portal/nrcs/detail/soils/survey/?cid=nrcs142p2_053627
- Ozdogan, M., and M. Rodell (2010), Simulating the effects of irrigation over the United States in a land surface model based on satellite-derived agricultural data, *J.*
- Rodell, M., D. Mocko, and H. K. Beaudoin (2015), LDAS: Land Data Assimilation Systems, Available from: <http://ldas.gsfc.nasa.gov/index.php>
- Rush, F. E., and V. R. Hill (1972), Bathymetric reconnaissance of Topaz Lake, Nevada and

California, *Water Resour. Inf. Ser. Rep.*

- Schulze, E. D., O. L. Lange, U. Buschbom, L. Kappen, and M. Evenari (1972), Stomatal responses to changes in humidity in plants growing in the desert., *Planta*, 108(3), 259–70, doi:10.1007/BF00384113.
- Serbina, L. O., and H. M. Miller (2014), *Landsat and water: case studies of the uses and benefits of landsat imagery in water resources*, US Geological Survey.
- Snyder, D. T., J. C. Risley, and J. V. Haynes (2012), *Hydrological information products for the Off-Project Water Program of the Klamath Basin Restoration Agreement*, US Geological Survey.
- Szilagyi, J., and A. Schepers (2014), Coupled heat and vapor transport: The thermostat effect of a freely evaporating land surface, *Geophys. Res. Lett.*, 41(2), 435–441, doi:10.1002/2013GL058979.
- Tasumi, M., and R. G. Allen (2007), Satellite-based ET mapping to assess variation in ET with timing of crop development, *Agric. Water Manag.*, 88(1), 54–62, doi:10.1016/j.agwat.2006.08.010.
- Tasumi, M., R. G. Allen, R. Trezza, and J. L. Wright (2005), Satellite-based energy balance to assess within-population variance of crop coefficient curves, *J. Irrig. Drain. Eng.*, 131(1), 94–109.
- Tasumi, M., R. G. Allen, and R. Trezza (2008), At-surface reflectance and albedo from satellite for operational calculation of land surface energy balance, *J. Hydrol. Eng.*, 13(2), 51–63.
- Temesgen, B., R. G. Allen, and D. T. Jensen (1999), Adjusting temperature parameters to reflect well-watered conditions, *J. Irrig. Drain. Eng.*, 125(1), 26–33.
- Tolk, J. A., and T. A. Howell (2001), Grain Sorghum Grown with Full and Limited Irrigation in Three High Plains Soils, *Trans. ASAE*, 44(6), 1553–1558.
- Truckee-Carson Irrigation District (2010), *Truckee-Carson Irrigation District Newlands Project Water Conservation Plan*, Truckee-Carson Irrigation District.
- USDA Farm Service Agency (2012), *Common Land Unit*, U.S. Department of Agriculture.
- USDA National Agricultural Statistics Service, and U. N. A. S. Service (2015), 2014 STATE AGRICULTURE OVERVIEW - Nevada, Available from: http://www.nass.usda.gov/Quick_Stats/Ag_Overview/stateOverview.php?state=NEVADA (Accessed 15 May 2015)
- Vidler Water Company (2015), VIDLER | Nevada, Available from: <http://www.vidlerwater.com/nevada.html>

Yan, L., and D. Roy (2016), Conterminous United States crop field size quantification from multi-temporal Landsat data, *Remote Sens. Environ.*

Appendix: Tables of Monthly Evapotranspiration

Table 4 – Monthly evapotranspiration for the Mason Valley study area for the years of study.

Monthly Evapotranspiration, in millimeters													
STUDY AREA	YEAR	JAN	FEB	MAR	APR	MAY	JUN	JUL	AUG	SEP	OCT	NOV	DEC
Mason Valley	2001	No Data	No Data	No Data	86.27	159.83	167.18	159.16	142.26	97.92	57.02	19.60	6.39
Mason Valley	2002	21.95	33.47	39.95	94.30	142.36	158.67	157.24	133.95	101.13	52.65	33.86	13.36
Mason Valley	2003	7.38	19.64	63.22	85.51	133.44	173.30	168.51	135.61	109.25	62.35	17.47	8.73
Mason Valley	2004	6.95	19.94	61.98	107.42	154.95	172.26	177.79	139.40	101.79	48.06	22.20	6.10
Mason Valley	2005	2.88	14.49	68.64	101.28	146.58	155.75	155.90	109.06	92.58	70.83	43.25	12.64
Mason Valley	2006	11.78	31.45	73.61	134.83	162.77	172.88	183.60	164.31	121.55	68.02	43.46	16.90
Mason Valley	2007	13.60	30.04	45.46	74.35	135.93	155.79	187.45	154.63	88.25	58.79	21.93	7.80
Mason Valley	2008	3.30	11.00	55.15	95.76	113.91	166.23	181.51	156.07	103.93	50.05	10.34	5.03
Mason Valley	2009	13.03	34.52	50.58	92.88	154.22	136.95	162.80	129.51	105.59	61.87	37.88	9.24
Mason Valley	2010	9.43	20.88	52.86	84.58	104.02	140.39	172.93	132.91	94.23	66.01	23.72	6.06
Mason Valley	2011	6.85	22.25	50.38	100.26	154.27	163.82	181.68	149.91	115.65	63.51	30.01	9.70

Table 5 – Monthly evapotranspiration for the Fallon study area for the years of study.

Monthly Evapotranspiration, in millimeters													
STUDY AREA	YEAR	JAN	FEB	MAR	APR	MAY	JUN	JUL	AUG	SEP	OCT	NOV	DEC
Fallon	2001	No Data	No Data	No Data	66.42	133.10	153.85	160.65	140.25	98.47	64.26	39.16	15.36
Fallon	2002	21.42	30.09	46.03	83.69	134.18	144.15	150.68	135.91	103.52	55.41	30.82	13.02
Fallon	2003	19.21	30.48	48.33	93.27	145.68	146.27	157.63	134.67	106.68	70.12	36.02	22.21
Fallon	2004	32.81	48.90	78.74	100.46	151.60	169.31	154.18	132.93	102.22	44.61	19.20	6.20
Fallon	2005	3.38	18.06	64.63	82.55	147.77	152.85	149.95	131.54	91.60	62.93	23.28	8.15
Fallon	2006	40.67	42.56	67.75	100.46	155.08	155.55	155.51	150.70	113.05	62.35	37.42	12.94
Fallon	2007	6.79	18.46	45.01	67.54	109.42	143.16	182.06	154.89	100.57	59.49	25.11	8.73
Fallon	2008	8.02	29.16	85.85	112.39	107.13	149.78	163.22	154.76	98.93	49.22	24.42	10.68
Fallon	2009	16.06	48.55	66.51	85.97	133.08	121.26	144.89	123.82	103.82	67.26	45.68	9.18
Fallon	2010	13.01	37.94	127.66	182.34	148.43	158.78	175.72	139.34	93.25	55.45	29.17	19.07
Fallon	2011	9.18	34.83	73.78	99.76	134.68	156.33	169.85	146.77	109.15	58.59	25.91	8.28

Table 6 – Monthly evapotranspiration for the Lovelock study area for the years of study.

Monthly Evapotranspiration, in millimeters													
STUDY AREA	YEAR	JAN	FEB	MAR	APR	MAY	JUN	JUL	AUG	SEP	OCT	NOV	DEC
Lovelock	2001	No Data	No Data	No Data	73.48	209.02	173.37	170.38	141.95	73.75	75.47	37.53	14.82
Lovelock	2002	16.15	32.67	44.11	73.45	130.12	132.91	159.46	125.10	90.51	46.22	35.16	13.93
Lovelock	2003	15.19	29.65	46.31	40.72	128.89	138.35	172.45	123.72	81.39	58.70	12.79	5.84
Lovelock	2004	3.63	13.76	60.35	71.85	91.40	117.67	100.93	79.46	62.30	31.92	9.57	2.94
Lovelock	2005	1.46	5.59	26.76	68.21	123.01	134.31	191.00	192.59	105.06	56.29	21.79	4.89
Lovelock	2006	22.82	61.25	78.04	111.59	178.22	171.88	183.29	152.71	111.15	74.69	39.32	12.74
Lovelock	2007	10.55	33.79	64.78	84.75	147.50	186.15	191.05	149.94	106.27	70.46	31.98	7.05
Lovelock	2008	9.61	48.94	105.75	157.05	168.91	177.11	222.95	169.18	108.43	66.78	37.83	10.26
Lovelock	2009	3.90	14.79	42.20	78.68	147.15	121.33	173.55	146.53	126.62	73.41	25.95	5.75
Lovelock	2010	17.90	109.26	95.78	89.79	130.22	141.87	173.02	131.64	102.92	79.29	28.30	9.72
Lovelock	2011	2.41	7.48	23.36	38.90	64.36	84.52	100.73	75.74	53.38	39.78	13.43	2.91

Table 7 – Monthly evapotranspiration for the Fish Springs Ranch study area for the years of study.

Monthly Evapotranspiration, in millimeters													
STUDY AREA	YEAR	JAN	FEB	MAR	APR	MAY	JUN	JUL	AUG	SEP	OCT	NOV	DEC
Fish Springs Ranch	2001	No Data	No Data	No Data	53.51	123.78	152.17	168.14	171.80	118.10	67.32	17.37	5.26
Fish Springs Ranch	2002	29.16	45.29	65.22	90.88	138.93	204.53	188.99	150.21	139.83	77.54	23.59	6.92
Fish Springs Ranch	2003	7.99	29.19	76.64	80.35	164.54	206.52	197.13	159.05	122.63	66.28	23.00	8.02
Fish Springs Ranch	2004	11.80	33.74	73.23	108.41	145.77	164.59	177.06	151.62	110.83	75.66	27.72	6.17
Fish Springs Ranch	2005	3.27	17.76	81.90	105.81	128.32	151.81	118.91	82.57	74.70	54.14	26.34	6.85
Fish Springs Ranch	2006	7.32	18.62	39.22	83.25	167.77	129.24	139.17	103.11	62.46	41.21	26.85	12.00
Fish Springs Ranch	2007	10.36	29.70	72.77	86.36	114.93	105.83	98.81	112.07	97.51	56.00	20.57	7.33
Fish Springs Ranch	2008	4.41	13.12	42.04	74.15	138.92	193.98	77.13	47.42	52.59	24.60	7.80	4.21
Fish Springs Ranch	2009	5.01	12.59	31.84	42.60	37.37	24.58	30.71	35.65	39.75	31.15	15.66	2.62
Fish Springs Ranch	2010	8.48	18.40	45.96	60.16	79.91	70.52	71.45	43.28	41.19	77.65	34.10	8.59
Fish Springs Ranch	2011	4.19	8.44	16.43	29.18	45.97	60.25	69.03	52.42	43.68	32.37	16.31	6.51